

**RESEARCH ARTICLE**

WILEY

A statistical comparison of spatio-temporal surface moisture patterns beneath a semi-natural grassland and permanent pasture: From drought to saturation

Ethan E. Wallace | Nick A. Chappell

Lancaster Environment Centre, Lancaster University, Lancaster, UK

Correspondence

Ethan E. Wallace, Lancaster Environment Centre, Lancaster University, Lancaster, UK.
Email: e.wallace@lancaster.ac.uk

Funding information

Eden Rivers Trust, Grant/Award Number: CGE Project 50; European Regional Development Fund; Natural Environment Research Council, Grant/Award Number: NE/R004722/1

Abstract

Some 60% of the agricultural land in the UK is grassland. This is mostly located in the wetter uplands of the west and north, with the majority intensively managed as permanent pasture. Despite its extent, there is a lack of knowledge regarding how agricultural practices have altered the hydrological behaviour of the underlying soils relative to the adjacent moorland covered by semi-natural grassland. Near-surface soil moisture content is an expression of the changes that have taken place and is critical in the generation of flood-producing overland flows. This study aims to develop a pioneering paired-plot approach, producing 1,536 moisture measurements at each of the monitoring dates throughout the studied year, that were subsequently analysed by a comparison of frequency distributions, visual cum geostatistical investigation of spatial patterns and mixed-effects regression modelling. The analysis demonstrated that the practices taking place in the pasture (ploughing, re-seeding and drainage) reduced the natural diversity in moisture patterns. Compared to adjacent moorland, the topsoil dried much faster in spring with the effects requiring offset with moisture from slurry applications in summer. With the onset of autumn rains, these applications then made the topsoil wetter than the moorland, heightening the likelihood of flood-producing overland flow. During the sampling within one such storm event, the adjacent moorland was almost as wet as the pasture with both visibly generating overland flow. These contrasts in soil moisture were statistically significant throughout. Further, they highlight the need to scale-up the monitoring with numerous plot pairs to see if the observed highly dynamic, contrasting behaviour is present at the landscape scale. Such research is fundamental to designing appropriate agricultural interventions to deliver sustainable sward production for livestock or methods of mitigating overland-flow incidence that would otherwise heighten flood risk or threaten water quality in rivers.

Abbreviations: ANOVA, analysis of variance; AD, Anderson–Darling; API, antecedent precipitation index; BF, Brown–Forsythe; KS, Kolmogorov–Smirnov; MWW, Mann–Whitney–Wilcoxon; OM, organic matter; PP, Permanent Pasture; SOF, Saturation-excess Overland Flow; SNG, Semi-Natural Grassland; TDR, time-domain reflectometry; θ_v , volumetric wetness.

This is an open access article under the terms of the Creative Commons Attribution License, which permits use, distribution and reproduction in any medium, provided the original work is properly cited.

© 2020 The Authors. *Hydrological Processes* published by John Wiley & Sons Ltd.

KEYWORDS

agricultural water management, geostatistical analysis, grassland hydrology, linear mixed-effects regression analysis, natural flood-risk management, soil volumetric wetness

1 | INTRODUCTION

Grassland accounts for 60% of the total UK agricultural area, which is proportioned almost equally at 55% as agriculturally improved permanent pasture and 45% rough grazing on semi-natural grasslands (DEFRA, 2019). Both permanent pasture and semi-natural grassland (often referred to as open-moorland or 'unimproved' pasture) encompasses a large percentage of the UK uplands, providing sustenance to grazing livestock alongside other ecosystem services (Bengtsson et al., 2019; Hayhow et al., 2019; Lamarque et al., 2011; Morse, 2019). Historically, semi-natural grassland was converted into permanent pasture during the eighteenth and nineteenth century to increase agricultural output (Kain, Chapman, & Oliver, 2004; Whyte, 2006). Gilman (2002), O'Connell et al. (2004), Holden et al. (2007) and Wheeler et al. (2008) all note the lack of research into the hydrological functioning of semi-natural grassland, with Gilman (2002) directly stating that 'there is little or no experimental evidence to support theoretical studies' relating to the effects of semi-natural grasslands on flood risk. Consequentially, it remains unknown how converting upland semi-natural grassland into permanent pasture has altered soil moisture regimes that affect flood generation processes and drought resilience.

Very few upland UK studies have compared semi-natural grasslands to permanent pasture, with research operating at coarse-scale resolution without conducting paired-plot analysis, thus, observations and knowledge of hydrological processes at the plot-hillslope scale is lacking. Orr and Carling (2006) compared catchment scale flood risk within North-West England, commenting that transitioning from Heather (*Calluna vulgaris*) or scrub vegetation to drained pasture could increase downstream flood risk. Marshall et al. (2006) and Wheeler et al. (2008) similarly concluded, through hydrograph assessment, that a semi-natural grassland in mid-Wales, UK (Pontbren experimental site), had a damped flood response compared to improved pasture. Ockenden and Chappell (2008) noted that a measured plot of semi-natural grassland was significantly drier than a nearby improved pasture in the River Eden catchment (Cumbria, UK). McIntyre and Marshall (2010), at Pontbren, noted that semi-natural grassland tended to have a less flashy flood response than improved pasture. Gilman (2002) is the only UK study to compare permanent pasture to semi-natural grassland as a primary research objective. The study concluded that pasture reversion could reduce River Severn peak flows by 0.5–2%, and smaller channel peak flows by 2–4%, although acknowledged the lack of supporting studies with which to justify model values used to simulate changes. These studies emphasise a considerable research gap, justifying the need for a hydrological comparison of permanent pasture and semi-natural grassland in an upland UK landscape (Wheeler et al., 2008). Indeed, there is a global dearth

of studies relating to how livestock production alters the hydrological functioning of natural soils (Magliano et al., 2019).

A significant component of the catchment water budget is the soil volumetric wetness (θ_v), which is the total volume of water present between soil particles divided by the total undisturbed soil volume. Soil θ_v is crucial in regulating hydrological system functioning (Gilman, 2002; Schulte et al., 2012). Antecedent θ_v preceding storm events can dictate rainfall–runoff responses by changing the likelihood of Saturation-excess Overland Flow (SOF) generation, even from highly permeable soils, so elevating both flood risk and water-quality degradation (Dunne & Black, 1970; Entekhabi, Rodriguez-Iturbe, & Castelli, 1996; Marshall et al., 2009; Minet, Laloy, Lambot, & Vanclooster, 2011). The precise spatial arrangement of θ_v is fundamental in determining a rainfall–runoff response, as purely using θ_v probability distributions does not capture spatial structures and therefore contributory area connectivity (Bonell & Williams, 1986; Grayson & Blöschl, 2000; Meijles, Dowd, Williams, & Heppell, 2015; Minet et al., 2011; Zehe & Blöschl, 2004). Soil θ_v is equally important during drought, determining water stress for agricultural crops, wildfire frequency etc. (Albertson, Ayles, Cavan, & McMorrow, 2009; Schulte et al., 2012). The spatial arrangement of θ_v during dry conditions can allow targeted irrigation (including slurry application) during water stress. An understanding of differences in spatio-temporal θ_v between semi-natural grassland and permanent pasture would, therefore, provide insights into the hydrological functioning of each land-use, and, therefore, infer how land conversion (or restoration) affects hydrological responses.

The aim of this study is to compare the spatio-temporal dynamics of surface soil volumetric wetness in an area of semi-natural grassland with an adjacent area that has been converted and managed as permanent pasture in the UK uplands. Both the reference and converted plots are adjacent to minimise natural differences. The methodological development aspect of the research aims to quantify the spatial variability of θ_v at the plot scale, which demands intense measurements. The research specifically measures each plot temporally, rather than the replication of plot pairs in the landscape, which is beyond the scope of this study. The plot comparison is conducted over a 6-month period (including drought and fully-saturated conditions), to assess non-stationarity in the differences. A high-resolution (1 m²) volumetric wetness grid (1,536 m²) was needed to capture fine-scale spatio-temporal soil moisture variability, which is then compared with localised factors such as land-use, vegetation, season, and elevation, to assess their impact.

Thus, the detailed research objectives are:

1. To develop a statistically robust methodology for the quantification of soil moisture differences between an example 768m² area

- of semi-natural grassland and an adjacent area of the same size managed as permanent pasture.
- To statistically contrast the volumetric wetness probability density functions between a permanent pasture and a semi-natural grassland, to quantify soil moisture differences.
 - To compare geostatistically the spatial structure of soil volumetric wetness between a permanent pasture and a semi-natural grassland, to assess spatially dependent soil moisture patterns.
 - To determine which factors significantly influence volumetric wetness in the contrasting, adjacent land-uses, to highlight any potential predictors of volumetric wetness at this particular locality.

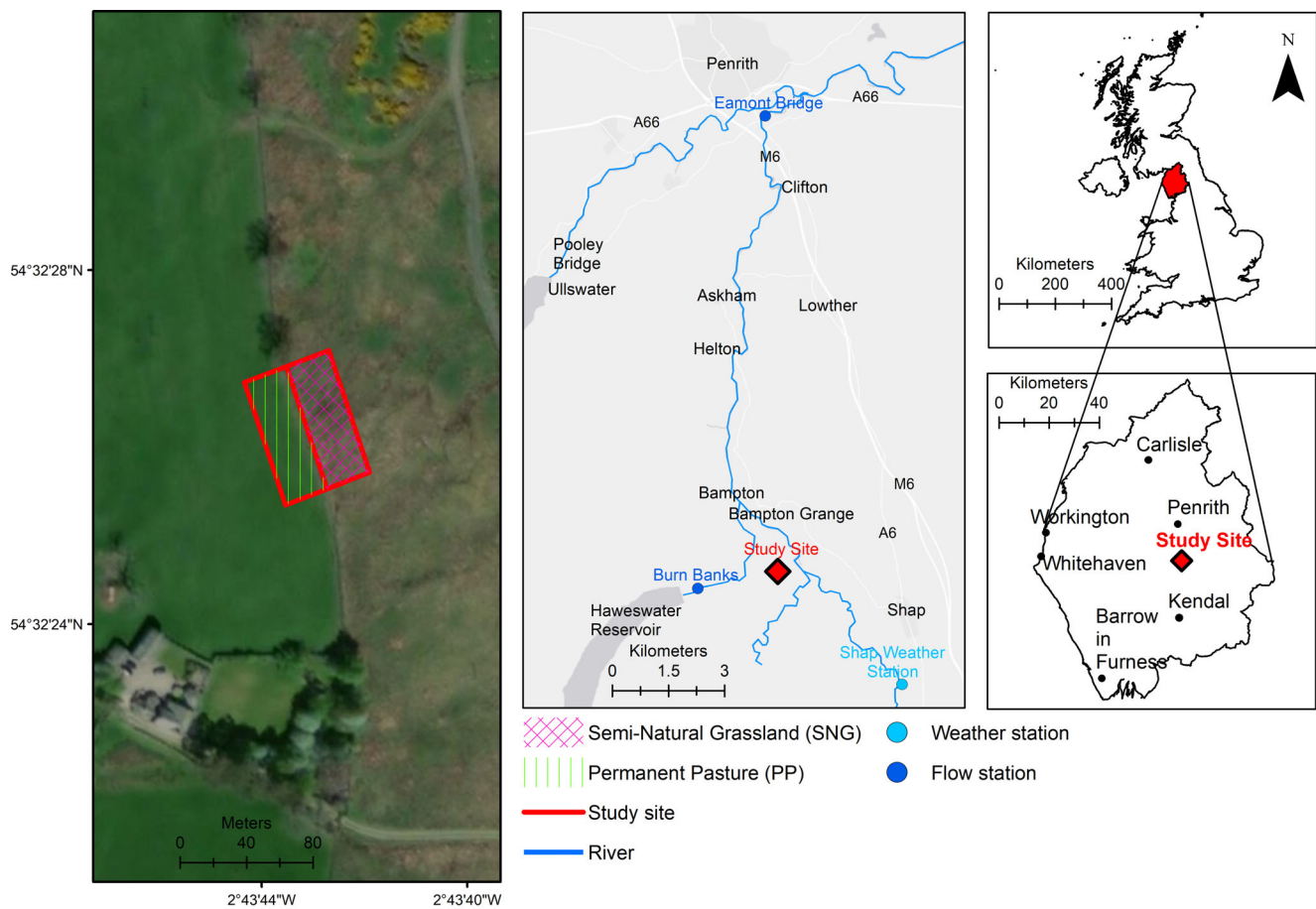
2 | MATERIALS AND METHODS

2.1 | Study site

Measurements were taken within a permanent pasture and a bordering semi-natural grassland located within the Lowther catchment,

3 km northwest of Shap (Cumbria, UK), between April 2018 and May 2019. The pasture (centre $54^{\circ} 32' 26''$ N, $2^{\circ} 43' 44''$ W) and semi-natural grassland (centre $54^{\circ} 32' 26''$ N, $2^{\circ} 43' 42''$ W) are immediately adjacent and are separated by a 1.3 m drystone wall (Figure 1). The drystone wall was likely raised between 1838 and 1855 based on surrounding Enclosure Acts (Kain et al., 2004; Whyte, 2006). Both plots are mapped as Brickfield Soil Association (Jarvis et al., 1984). This equates to an FAO Eutric Stagnosol, or an Aquic soil within several USDA soil orders (USDA, 1999; WRB, 2015). Eutric Stagnosols are widespread throughout the UK uplands, and are highly susceptible to saturation, poor drainage, and overland flow (Jarvis et al., 1984). The study site soils are till derived and slowly permeable, which overlay Tarn Moor Formation mudstone of the Buttermere and Bitter Beck Formations within the Skiddaw Group (Cooper et al., 1995; Stone, 2007).

The local climate from the Shap weather station ($54^{\circ} 30' 49''$ N, $2^{\circ} 40' 40''$ W: 301 masl: Figure 1) is wet temperate, with a mean winter temperature of 4.1°C , a mean summer temperature of 11.5°C , and an annual rainfall average of 1,779 mm (Met



Contains OS data © Crown copyright and database right (2020).

FIGURE 1 The experimental site within a UK, Cumbrian, and local area context. The permanent pasture (PP) and semi-natural grassland (SNG) sites are highlighted in green stripes and pink crosshatch, respectively. Shap weather station, alongside the downstream river gauging station (Eamont Bridge), is shown. Historically, the pasture was semi-natural grassland until being improved during the Inclosure (Enclosure) Acts of the early-mid 19th century, with the wall likely erected between 1838-1855. The site is within a headwater where downstream settlements such as Penrith, Eamont Bridge and Carlisle suffer from flooding

Office, 2020). Daily precipitation data alongside downstream River Lowther discharge (gauged at Eamont Bridge; 54° 38' 60" N, 2° 44' 15" W; 119 masl; Figure 1) during the study is given in Figure 2. An Antecedent Precipitation Index (API) for the study site (Figure 2) was calculated according to Equation ((1)):

$$API_t = R_t + \kappa API_{t-1} \quad (1)$$

where API is the antecedent precipitation index, R is the daily precipitation total and κ is an empirical decay factor below 1. A κ value of 0.99 was chosen for this site as catchment conditions change relatively slowly and the API covered almost a full year. An initial condition ($API_{t=0}$) of 450 was approximated for mid-December 2017, which had no affect beyond April 2018, with the experiment beginning in May 2018.

The Permanent Pasture (PP) is a re-seeded agriculturally improved pasture dominated by ryegrass (*Lolium spp.*) and clover (*Trifolium spp.*), but with ingress of common rush (*Juncus effusus*). PP is moderately grazed by both sheep (7.4/ha) and beef cattle (0.5/ha), averaging approximately 1.4 grazing livestock units per ha. The pasture receives sporadic slurry, fertiliser and lime application, as well as infrequent mechanical soil loosening as part of typical regional farming practice, although the latter did not occur during the experiment. The PP plot is well separated from farm tracks and field gates and does not receive surplus vehicular passes, or excessive trampling or grazing pressure in comparison to the remaining pasture. Sections of the PP field are drained.

The Semi-Natural Grassland (SNG) plot on Ralpland Common is communally grazed at moderate intensity by sheep (0.6/ha), with occasional grazing by a small population of wild red deer (*Cervus elaphus*). The area is a "rush pasture" of predominantly common rush and includes a wide variety of vegetation species that are primarily controlled by grazing. Management of SNG is minimal, with no evidence of burning, quarrying, peat extraction, drainage, or other intensive management practice. The studied SNG area is separated from local vehicle and walking tracks, only receiving infrequent quadbike passes during shepherding.

2.2 | Experimental design

A paired-plot experimental design was adopted as PP and SNG are immediately adjacent Eutric Stagnosols with similar slopes (4–4.5%). Both PP and SNG have virtually identical distributions of topographic wetness (Figure 3). Both plots were covered by semi-natural grassland until PP was enclosed, likely during the early-mid 19th century (Kain et al., 2004). This experimental design therefore suggests observed differences are due to land conversion and subsequent management as opposed to inherent site dissimilarity. The study site location was appropriate due to PP and SNG belonging to the most common upland soil type in England, with both sites following typical regional pastoral/moorland agricultural practice. Supporting precipitation and discharge information was available to infer site conditions prior to and between sampling and to aid interpretation of results. Given that frontal rainfall is the dominant precipitation mechanism in the UK,

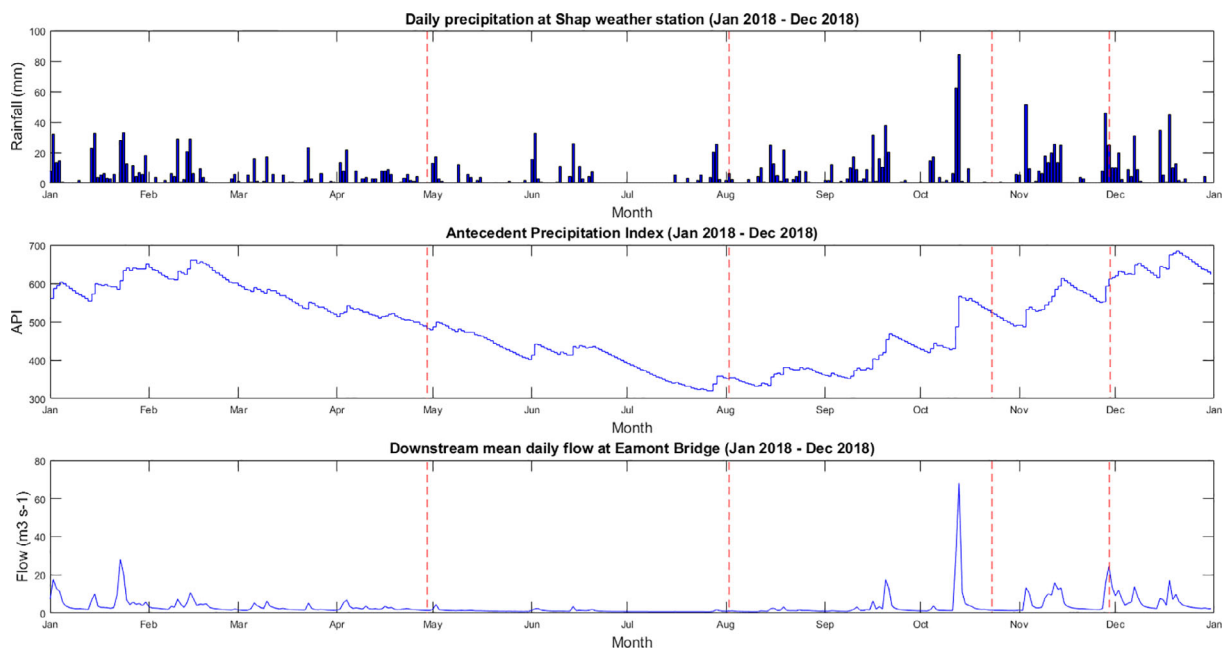
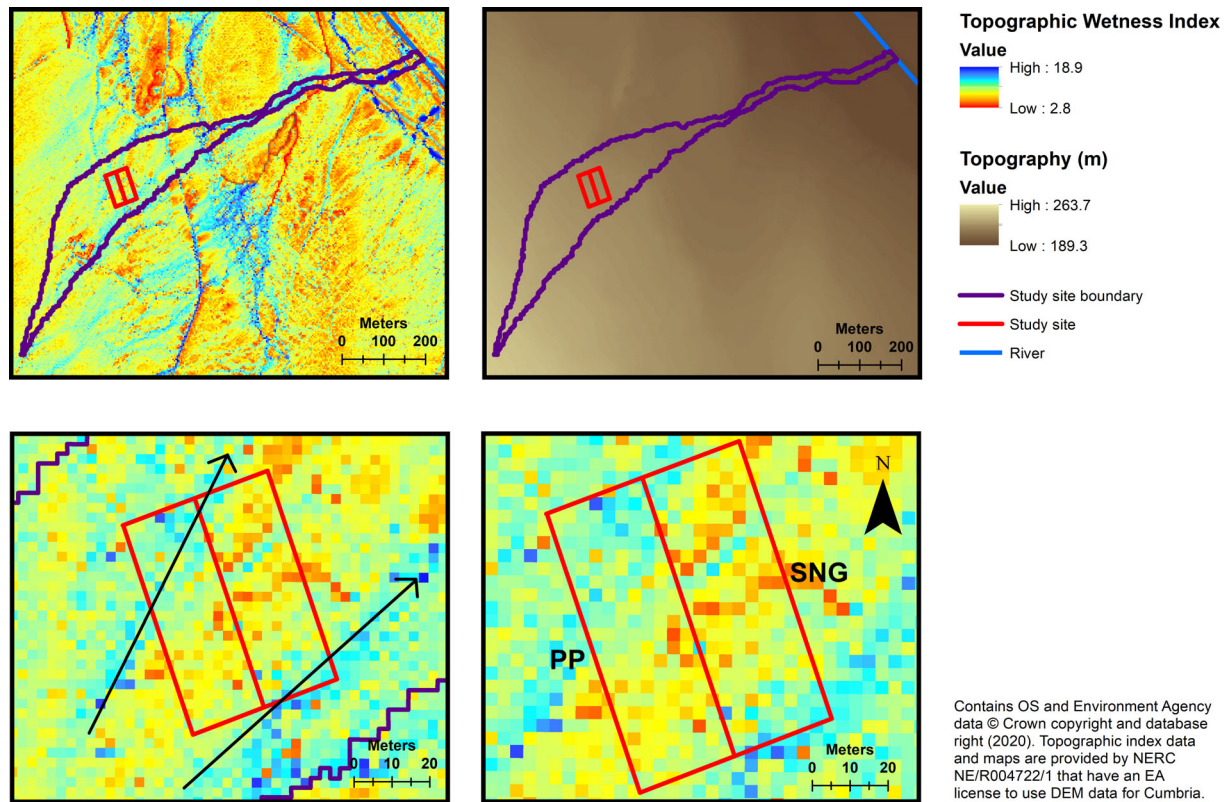


FIGURE 2 The daily precipitation data taken from Shap weather station throughout the experiment, alongside the Antecedent Precipitation Index (API) and the mean daily downstream flow at Eamont Bridge (see Figure 1). The sampling dates and API for 29th May (407), 2nd August (355), 23rd October (524) and 29th November (611) are shown (red dash), respectively. Note that the hydrological record covers the 2018 British Isles heatwave that lasted from 22nd June to 7th August. Precipitation data is provided by Gaugemap (2019), and discharge data by EA (2019)



Contains OS and Environment Agency data © Crown copyright and database right (2020). Topographic index data and maps are provided by NERC NE/R004722/1 that have an EA license to use DEM data for Cumbria.

FIGURE 3 The topographic wetness index (Kirkby index) for both the Permanent Pasture (PP) and the Semi-Natural Grassland (SNG). The topographic wetness index is calculated according to $\ln(\alpha/\tan\beta)$, where α is the local upslope area draining through a certain point per unit contour length, and β is the local slope angle in radians. Note that both PP and SNG have similar upslope drainage areas, and similar slopes, and hence, very similar distributions of topographic wetness. Arrows have been annotated over the bottom-left figure to highlight the dominant flow-paths travelling through the paired-plots. The depression that retains moisture within the centre of the SNG plot (see figures 9-11) is also clearly visible within the bottom-right figure

TABLE 1 The timetable for volumetric wetness, terrain, soil and vegetation sampling

| Date | Activity |
|-------------------|------------------------------|
| 29/05/18 | Volumetric wetness sampling |
| 02/08/18 | Volumetric wetness sampling |
| 23/10/18 | Volumetric wetness sampling |
| 29/11/18 | Volumetric wetness sampling |
| 12/03/19–13/03/19 | Terrain sampling |
| 14/05/19 | Vegetation and soil sampling |

both plots are assumed to have identical hydrometeorological inputs. Sheltering from the drystone wall is assumed minimal.

A rectangular 32 m by 48 m (1,536 m²) sampling grid encompassing both land-uses equally was used to measure volumetric wetness (θ_v) at a 1 m resolution. This grid size was deemed the maximum number of point measurements that could be collected without the grid wetting/drying during sampling. The combined 1,536 samples were considered sufficient for statistical modelling. Soil θ_v was measured four times over a six-month period (Table 1), spanning from drought to fully saturated conditions. Fixed markers remained, but the grid of measuring tapes was removed following each sampling date to

avoid inhibiting agricultural practices. Following the final θ_v sampling, relative elevation and vegetation composition were recorded at an identical 1 m resolution to support interpretations.

This intensive sampling regime collected more results than any previous plot study of θ_v on grassland in the UK. For example, Meijles, Williams, Ternan, and Dowd (2003) recorded moisture at 151 locations over a 12,000 m² plot, and Ockenden and Chappell (2008) used a range of sampling intensities from 101 locations over a 525 m² plot to 546 locations over a 4,000 m² plot. The greater sampling intensity in this study was considered important to ensure accurate frequency distributions and so accurate summary statistics; visual representation of soil moisture patterns and quantitative estimates of the spatial structure (via empirical semi-variograms and models of these); and credible comparison of the moisture patterns with some of the potential controlling factors.

2.2.1 | Surface volumetric wetness measurement (0–6 cm)

Topsoil volumetric wetness was measured in situ in the field during each sampling date. A moisture probe (ML3 'Theta-probe': Delta-T Devices Ltd) gave 768 readings per land-use for each sampling date (1,536 total). The device consists of four 6 cm waveguides arranged in

a trefoil formation (attached to a probe body) that was fully inserted into the soil surface. This moisture probe measures θ_V (m^3/m^{-3}) using a simplified version of time-domain reflectometry (TDR). In brief, the moisture probe emits a continuous 100 MHz outgoing wave and records the reflection of this wave to produce a composite standing wave. The outgoing and standing wave ratio is dependent upon the dielectric constant of the soil surrounding the waveguides, which is largely controlled by θ_V (see Gaskin & Miller, 1996). Simplified TDR was the selected experimental method due to it being a rapid and repeatable in-field technique (see Gaskin & Miller, 1996).

Following Whalley (1993), the moisture probe reported in-field measurements in millivolts (mV), which were converted to θ_V post-measurement via the calibration equation (Equation (2)):

$$\theta_V = \frac{[1.07 + 6.4mV - 6.4mV^2 + 4.7mV^3] + \alpha_0}{\alpha_1} \quad (2)$$

where α_0 and α_1 are soil coefficients and were taken as -1.6 and $+8.4$, respectively, due to the experiment primarily involving mineral soils (Whalley, 1993). The moisture probe is accurate to $\pm 2\%$ θ_V and averages θ_V over the full length of the waveguides, primarily around the central waveguide (Gaskin & Miller, 1996; Whalley, 1993). The same moisture probe was used for all measurements to account for any unknown instrument bias. Gaskin and Miller (1996) and Miller, Gaskin, and Anderson (1997) give detailed information regarding the design, operation, calibration and uncertainty of moisture-probe measurements.

2.2.2 | Reference topsoil physio-chemical properties which may influence volumetric wetness

Several large-scale studies have shown that soil physio-chemical properties can substantially influence soil θ_V (e.g., Pan, Boyles, White, & Heitman, 2012). Soil texture (Wallace & Chappell, 2019), porosity (Beven & Germann, 1982), acidity (Holland et al., 2018), bulk density (Drewry, Littlejohn, & Paton, 2000), penetration resistance (Wallace & Chappell, 2019) and organic matter content (Beven & Germann, 1982) can all affect soil structural stability and functioning, and therefore permeability and water retention. To determine such properties, topsoil was extracted from the surface 10 cm. Soil samples were taken using 221 cm^3 bulk density tins across 16 randomly selected locations throughout PP and SNG (Figure 4). Random sampling was chosen as it eliminated sampling bias. Four soil samples per location were taken, with three undergoing an initial 48-hour air dry. The first air-dried sample was used to measure soil pH. The second air-dried sample was oven dried at $105^\circ C$ for 24 hr for dry bulk-density calculation, and then underwent a 6-hr $550^\circ C$ loss-on-ignition test to calculate organic matter (OM). The third air-dried sample underwent particle size analysis. Particle size analysis involved sieving oven dried soil through a 2000- μm sieve, before mixing the sample with 1% sodium poly-metaphosphate for 24 hours to separate aggregates. The soil then underwent hydrogen peroxide treatment to remove organic material. Finally, samples underwent manual aggregate breaking and high-

power sonication for 5 min before laser diffraction (Beckman Coulter, LS-13-320). The final sample was gradually submerged for 48 hr with de-ionised water and was then measured with the moisture probe to determine soil porosity (i.e., maximum volumetric wetness) to remain consistent with field measurements. Soil penetration resistance was measured in situ adjacent to soil sampling locations, using an SC900 Field Scout (Spectrum Technologies) penetrometer using a 12.8 mm diameter cone. The device measures soil penetration resistance via an internal load cell and uses an ultrasonic depth sensor to record depth in 2.5 cm steps for up to 7.5 cm.

2.2.3 | Correlating terrain and vegetation properties with soil volumetric wetness

A 1 m resolution topographic survey of the site was undertaken four months after the θ_V sampling, as topography may influence soil θ_V patterns (following Meijles et al., 2015; Meijles, Williams, Ternan, Anderson, & Dowd, 2006; Minet et al., 2011). The terrain survey combined a differential GPS (Trimble R8-Integrated GNSS) with a total station (Trimble, Robotic-S6), giving both the coordinates and elevation of each point. A vegetation survey followed the terrain analysis to allow θ_V to be compared against floristic composition. Vegetation potentially explains a significant amount of θ_V variance within areas of (semi-)natural vegetation (Chappell & Ternan, 1992; Meijles et al., 2003). The genera/species that encompassed the majority of the above-surface biomass in each square metre was recorded, even if several were present. Each square metre was centred around a TDR measurement point. The vegetation survey occurred 6 months following θ_V sampling during mid-Spring to aid vegetation identification. No taxonomic shifts were evident throughout the experiment, and thus, vegetation communities were assumed stationary.

2.3 | Statistically analysing and modelling volumetric wetness

2.3.1 | Comparing volumetric wetness distributions (objective I)

Soil θ_V distributions at each sampling date were assessed for normality via Kolmogorov-Smirnov (KS) and Anderson-Darling (AD) tests. Theoretically, θ_V distributions cannot satisfy normality due to the bounding effect of porosity (which distorts frequency distributions into substantial negative skews), although normality can be an adequate practical assumption (Western, Grayson, & Blöschl, 2002). Soil θ_V distributions underwent Box-Cox transformations for further normality assessment.

Untransformed θ_V distributions were compared between land-uses via the non-parametric Mann-Whitney-Wilcoxon (MWW) test to avoid normality assumptions. Homogeneity of variances was tested via the non-parametric Brown-Forsythe (BF) test (Brown & Forsythe, 1974). The non-parametric statistical approaches justify the

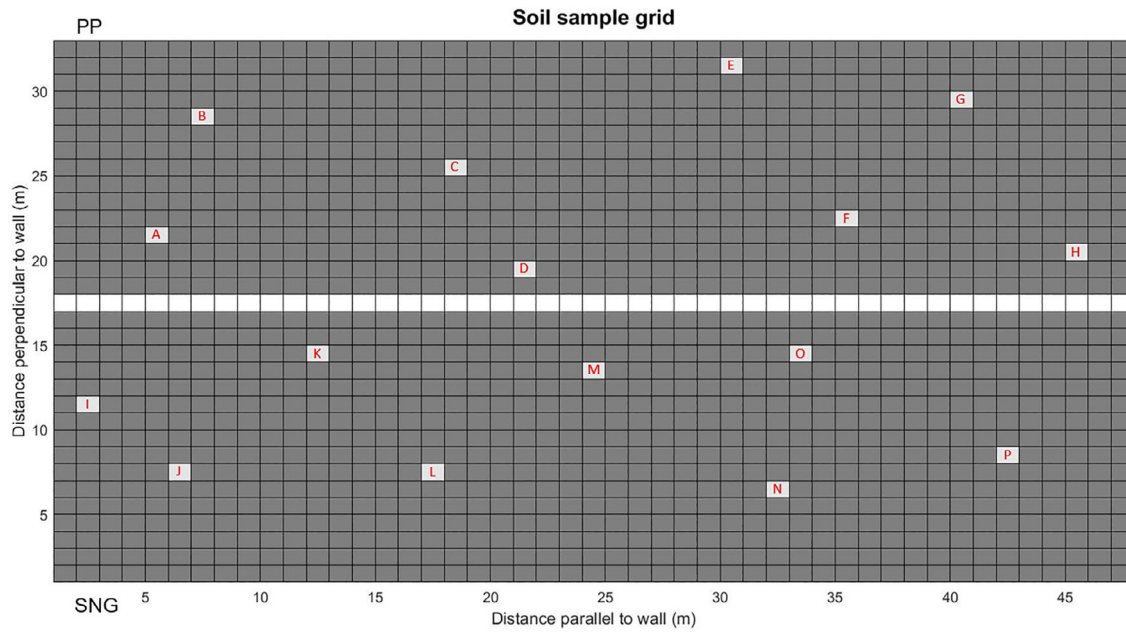


FIGURE 4 Labelled topsoil sample locations within the Permanent Pasture (PP: top) and Semi-Natural Grassland (SNG: bottom) taken on the 14th May 2019. The drystone-wall is also shown to separate the land-uses

need for such an intensive sampling regime. Significance levels were taken as $p \leq .05$, $p \leq .01$ and $p \leq .001$.

2.3.2 | Volumetric wetness spatial structure (objective II)

The GLOBEC geostatistical package in MATLAB (Chu, 2017) was used to generate empirical semi-variograms from θ_V observations, to assess PP and SNG spatial structure. Semi-variogram models were derived using the GLOBEC least-square fit function. A range of models were fitted to the empirical semi-variogram data, including exponential (Equation (3)), Gaussian (Equation (4)) and spherical (Equations (5.1) and (5.2)) models:

$$\gamma_{h_{exp}} = P_0 \left(1 - e^{-\left(\frac{h}{L}\right)} \right) + \gamma_0 \quad (3)$$

$$\gamma_{h_{gau}} = P_0 \left(1 - e^{-\left(\frac{h}{L}\right)^2} \right) + \gamma_0 \quad (4)$$

$$\gamma_{h_{sph}} = P_0 \left(\frac{1.5h}{L} - \frac{1.5h^3}{L^3} \right) + \gamma_0, 0 < h \leq L \quad (5.1)$$

$$\gamma_{h_{sph}} = P_0 + \gamma_0, h > L \quad (5.2)$$

where γ_h is semi-variance at each lag distance, P_0 is the partial sill, h is the lag distance, L is the length scale and γ_0 is the nugget effect. A residual sum of squares gave a goodness of fit for each semi-variogram model.

2.3.3 | Relative influence of potential controlling variables on observed volumetric wetness patterns (objective III)

To correlate elevation with soil θ_V , the *corrcoef* function in MATLAB was used. The influence of flora was assessed by comparing dominant genera/species with soil θ_V values. To assess if each recorded variable significantly influences θ_V , a linear mixed-effects regression model was developed using the *lmer* function within the *lme4* package (Bates, Maechler, & Bolker, 2012) using R statistical programming (R Core Team, 2018). A linear mixed-effects regression approach was necessary due to the hierarchical, highly auto-correlated, non-independent nature of the investigated variables, alongside the possibility of including temporal changes and repeat measurements within the model. Stepwise bidirectional elimination utilising a combination of Akaike and Bayesian Information Criteria created the most parsimonious model to account for soil θ_V variance. Soil θ_V was predicted according to fixed effects of land-use, month, and vegetation, with interaction effects of month-vegetation and month-land-use. Random effects were taken as the intercept of elevation, with by-elevation random slopes for the effect of month and vegetation. Elevation was taken as a random effect as a limited elevation range for the local area was taken, and elevation weakly correlated with θ_V . An analysis of variance (ANOVA) test using the ANOVA function was applied to the model summary to outline each explanatory factor significance (R Core Team, 2018). All linear mixed-effects regression model assumptions were satisfied following model calibration to ensure model suitability.

TABLE 2 The topsoil physio-chemical properties taken within the Permanent Pasture (PP) and the Semi-Natural Grassland (SNG) on the 14th May 2019 (Figure 4)

| Site | Particle-size distribution (%) | | | | | | Surface penetration resistance (kN) | | | | | | pH | Bulk density (g/cm ³) | OM (% weight) | η (%) |
|---------------|--------------------------------|--------------------|---------------------|----------------------|------------------------|-----------------|-------------------------------------|--------|---------|--------|--------|-----------|--------|-----------------------------------|---------------|------------|
| | $\leq 2 \mu\text{m}$ | 2–20 μm | 20–60 μm | 60–200 μm | 200–2000 μm | Soil texture | θ_v (%) | 0 cm | 2.5 cm | 5 cm | 7.5 cm | | | | | |
| A | 41.6 | 47.7 | 6.9 | 3.8 | 0.0 | Silty clay | 37.4 | 104 | 207 | 1,104 | 1,138 | 5.48 | 0.92 | 15.3 | 57.3 | |
| B | 36.0 | 41.6 | 9.1 | 13.3 | 0.1 | Silty clay loam | 34.3 | 586 | 1,311 | 794 | 932 | 6.08 | 1.00 | 13.6 | 58.5 | |
| C | 23.9 | 36.3 | 14.0 | 14.6 | 11.3 | Silt loam | 36.9 | 0 | 34 | 1,173 | 932 | 6.02 | 0.77 | 23.9 | 58.2 | |
| D | 32.7 | 50.9 | 10.3 | 6.1 | 0.0 | Silty clay loam | 31.9 | 242 | 1,346 | 1,346 | 1,138 | 5.91 | 0.77 | 18.1 | 57.4 | |
| E | 30.3 | 43.6 | 12.1 | 13.4 | 0.5 | Silty clay loam | 34.0 | 287 | 391 | 1,035 | 886 | 6.19 | 0.58 | 17.8 | 57.7 | |
| F | 20.0 | 39.9 | 17.0 | 15.1 | 8.4 | Silt loam | 35.7 | 207 | 862 | 862 | 862 | 6.25 | 0.81 | 13.9 | 58.3 | |
| G | 33.3 | 52.0 | 10.1 | 4.6 | 0.0 | Silty clay loam | 33.9 | 518 | 1,276 | 1,414 | 1,484 | 5.97 | 0.69 | 13.6 | 58.2 | |
| H | 28.3 | 42.8 | 12.8 | 15.4 | 0.8 | Silty clay loam | 36.8 | 207 | 1,380 | 1,208 | 1,173 | 5.85 | 0.95 | 13.6 | 58.5 | |
| I | 35.4 | 55.3 | 7.2 | 2.1 | 0.0 | Silty clay loam | 38.7 | 34 | 138 | 518 | 1,000 | 5.07 | 0.83 | 11.9 | 58.2 | |
| J | 25.5 | 44.1 | 16 | 14.2 | 0.3 | Silt loam | 39.1 | 0 | 104 | 276 | 276 | 4.94 | 0.76 | 12.7 | 59.8 | |
| K | 32.6 | 50.6 | 12.4 | 4.4 | 0.0 | Silty clay loam | 47.4 | 69 | 69 | 1,035 | 380 | 4.37 | 0.77 | 23.6 | 60.7 | |
| L | 24.7 | 37.2 | 11.1 | 19.7 | 7.3 | Loam | 50.7 | 518 | 380 | 345 | 276 | 5.24 | 0.44 | 27.8 | 59.9 | |
| M | 14.6 | 24.2 | 15.8 | 27.5 | 17.9 | Loam | 54.6 | 104 | 86 | 112 | 233 | 5.15 | 0.17 | 23.5 | 58.2 | |
| N | 16.7 | 24.0 | 15.2 | 28.9 | 15.2 | Loam | 58.0 | 34 | 104 | 207 | 69 | 5.42 | 0.60 | 62.3 | 61.1 | |
| O | 28.7 | 37.3 | 14.0 | 15.8 | 4.3 | Silty clay loam | 46.5 | 0 | 0 | 932 | 862 | 5.66 | 0.36 | 28.1 | 59.9 | |
| P | 29.4 | 33.8 | 13.9 | 14.5 | 8.4 | Clay loam | 42.6 | 0 | 0 | 1,484 | 1,449 | 4.69 | 0.53 | 16.9 | 58.3 | |
| PP \bar{x} | 31.5 | 43.2 | 11.2 | 13.4 | 0.3 | NA | 39.0 | 225 | 1,069 | 1,139 | 1,035 | 6.00 | 0.79 | 14.6 | 58.2 | |
| SNG \bar{x} | 27.1 | 37.3 | 14.0 | 15.2 | 5.8 | NA | 47.0 | 34 | 95 | 432 | 328 | 5.11 | 0.57 | 23.6 | 59.9 | |
| PP σ | 6.8 | 5.4 | 3.1 | 5 | 4.5 | NA | 1.9 | 197 | 562 | 217 | 209 | 0.24 | 0.14 | 3.6 | 0.5 | |
| SNG σ | 7.3 | 11.3 | 2.9 | 9.6 | 6.9 | NA | 7 | 175 | 120 | 485 | 481 | 0.41 | 0.23 | 16 | 1.1 | |
| MWW (p) | 0.235 | 0.279 | 0.246 | 0.279 | 0.333 | NA | <0.001*** | 0.038* | 0.006** | 0.041* | 0.027* | <0.001*** | 0.028* | 0.278 | 0.022* | |

Note: Variables included particle-size distribution, soil texture, soil volumetric wetness (θ_v), surface penetration resistance, pH, bulk density, organic matter (OM), and porosity (η). Variable medians (\bar{x}) are statistically compared via the non-parametric Mann–Whitney–Wilcoxon (MWW) test. *Significant at the 0.05 probability level. **Significant at the 0.01 probability level. ***Significant at the 0.001 probability level.

3 | RESULTS AND DISCUSSION

3.1 | Reference site conditions which may influence volumetric wetness

3.1.1 | Physio-chemical topsoil properties

Topsoil samples from PP and SNG (Figure 4) were compared to investigate physio-chemical properties, which may influence soil θ_v , and to contextualise findings (Table 2). Textural analysis reveals statistically similar distributions for all particle size fractions ($\leq 2 \mu\text{m}$, $2\text{--}20 \mu\text{m}$, $20\text{--}60 \mu\text{m}$, $60\text{--}200 \mu\text{m}$, $200\text{--}2000 \mu\text{m}$). The pasture topsoil (Figure 5) was predominantly silty-clay loam (62.5%), with some silt loam (25%) and silty-clay (12.5%). The semi-natural grassland topsoil (Figure 5) was mostly silty-clay loam (37.5%) and loam (37.5%), with some silt loam (12.5%) and clay loam (12.5%).

During topsoil sampling (Table 2), PP was significantly drier than SNG ($p \leq .001$), with a median θ_v of 39% as opposed to 47%. The pasture also had significantly higher soil penetration resistance ($p \leq .006\text{--}.041$) at all recorded depths (0, 2.5, 5 and 7.5 cm), partly due to the drier soil (Wallace & Chappell, 2019). Bulk density was significantly higher ($p \leq .028$) within the PP plot compared to the SNG plot, with porosity significantly lower ($p \leq .022$), possibly indicating that vegetation differences may have some influence upon soil properties (Macleod et al., 2013), or that agricultural practices had compacted the pasture and potentially reduced the infiltration capacity (Drewry et al., 2000; Gilman, 2002; Pan et al., 2012).

Both plots had statistically similar ($p \leq .278$) OM levels (Table 2). This may be because of slurry additions to the pasture that are maintaining the naturally high levels of OM seen in the soils beneath semi-natural grassland. Organic matter content was, however,

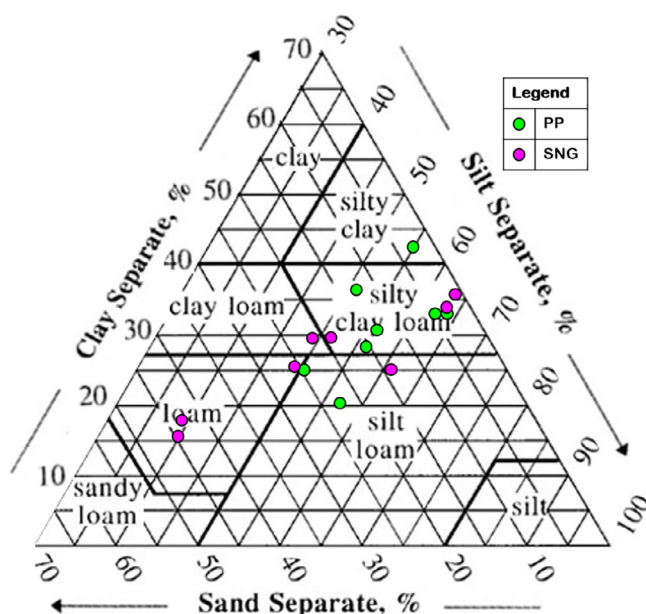


FIGURE 5 The soil particle-size analysis for the Permanent Pasture (PP) and the Semi-Natural Grassland (SNG)

considerably more variable within the SNG plot, likely due to the presence of localised carbon-rich 'rush flushes' within the Eutric Stagnosol (Chappell & Ternan, 1992). Indeed, sample point 'N' in SNG (Figure 4) contained more than 2.5 times the OM of the most organic PP sample. The PP plot was significantly less acidic than the SNG plot ($p \leq .001$), probably due to liming (Holland et al., 2018).

3.1.2 | Topography and elevation survey

The detailed topographic survey (Figure 6) showed that PP was marginally higher than SNG, with an arithmetic mean of 222.5 masl as opposed to 221.8 masl. Topography shows PP and SNG have similar elevation profiles. Average gradients perpendicular to the drystone wall are 4.3% for PP and 4.5% for SNG, whilst average gradients parallel to the drystone wall are 4% for PP and 4.1% for SNG.

Linear drainage features following a South-by-South-West to North by North-East (SSW-NNE) trajectory are visible in some moisture plots (refer to later Figures 9 & 11). The SSW-NNE connectivity of the near-surface drainage is most visible within the SNG plot, with agricultural interventions making this less clear within the PP plot. Both plots have a virtually identical topographic wetness (Figure 3), suggesting both plots should have similar θ_v values, and therefore differences in saturation should be predominantly due to land-use as opposed to landscape factors.

The foundations of the drystone wall may impede any shallow drainage of moisture from the PP plot to the SNG plot, giving accumulation upslope of the wall within PP. This effect is, however, not seen in the surface moisture measurements (refer to later Figures 9–12); perhaps indicating the walls foundation is permeable. Figure 6 highlights a shallow depression within the SNG plot beginning at the drystone wall at approximately 28 m North-West along the wall, heading approximately North-East. This depression is likely to retain moisture and may have contributed to the increased OM soil content as observed in sample point 'N' (Figure 4).

3.1.3 | Vegetation survey

The taxonomic survey (Figure 7) reveals a small number of dominant genera/species within each square metre. The PP plot was almost entirely dominated by ryegrass, encompassing 94.7% of the sampling grid, with pockets of common rush covering only 4.4%. Stinging nettle (*Urtica dioica*) and broad-leafed dock (*Rumex obtusifolios*) were present against the drystone wall, at 0.7 and 0.3% of the area, respectively. The pasture contained significant clover, buttercup (*Ranunculus spp.*) and ox-eye daisy (*Leucanthemum vulgare*) populations, likely from re-seeding mixtures, although these never dominated a grid cell.

Vegetation within SNG (Figure 7) was predominantly a mixture of the *Pooideae* subfamily of grass species (65.4%), primarily consisting of common bent (*Agrostis capillaris*), creeping bent (*Agrostis stolonifera*), mat-grass (*Nardus stricta*) and ryegrass. This grass mixture is hereby referred to as 'moorland grass'. Common rush was also very common at 33.6%. Stinging nettle and broad-leafed dock occurred at

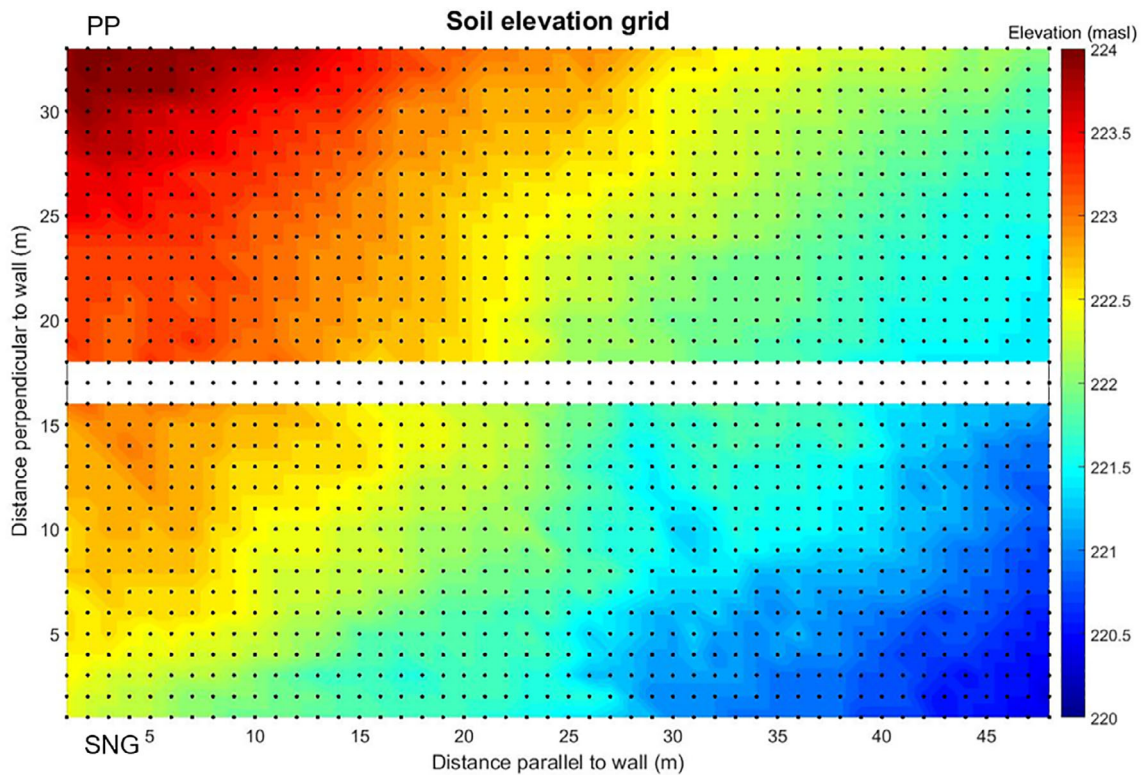


FIGURE 6 The elevation profile at the study site, within the Permanent Pasture (PP: top) and Semi-Natural Grassland (SNG: bottom). The wall separating the plots is approximately along a NNW-SSE axis. Note the depression at the boundary within SNG at approximately 28 m distance parallel to the wall, which extends further into SNG. It is likely this local depression will remain wetter than the surrounding areas throughout the experiment (see Figure 3)

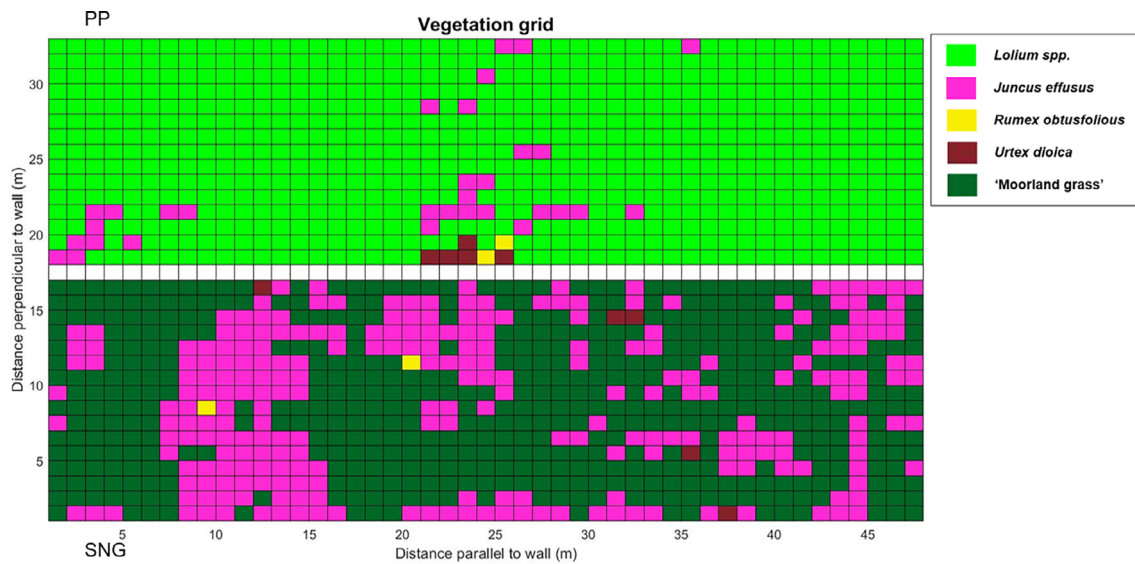


FIGURE 7 The dominant vegetation within each square metre, with the Permanent Pasture (PP: top) and Semi-Natural Grassland (SNG: bottom) highlighted. Note that SNG contains substantially more common rush, and that the moorland grass is an admixture of several different grass species. The stinging-nettle and broad-leaved dock within PP border the wall and are amassed around a small tree stump

0.7 and 0.3% incidence, respectively. A large number of additional vegetation species were recorded within SNG, particularly plume thistles (*Cirsium spp.*), and *Sphagnum* mosses (*Sphagnum spp.*), with no grid containing fewer than three species.

Ryegrass dominance within PP is due to pasture re-seeding to maintain sward levels and prevent reversion (Gilman, 2002), with the significant clover and ox-eye daisy population further supporting re-seeding. Common rush prevalence in both land-uses is likely caused

by locally poor drainage in a high rainfall environment, both highly suited to *Juncus* spp. proliferation (AHDB, 2013; McCorry & Renou, 2003). Gilman (2002) notes that *Juncus* spp. will often be the first moorland species to colonise ryegrass/clover swards in high rainfall upland environments of the UK. Nearby upland catchment studies have also noted considerable *Juncus* spp. and *Nardus* spp. compositions, both being typical of upland soils (Gilman, 2002; Orr & Carling, 2006).

To reemphasize, minimal research has compared the differences between moorland and pasture vegetation that may be correlated with changes in hydrological properties. Semi-natural grassland conversion likely reduced vegetation height, biomass and root depth, thereby reducing rainfall input due to wet-canopy evaporation, as well as soil porosity (Gilman, 2002; Orr & Carling, 2006; Sansom, 1999). Sansom (1999) and Gilman (2002) postulate that moorland conversion reduces infiltration rates, hydraulic conductivity, surface roughness and evapotranspiration, ultimately causing increased overland flow and elevated flood risk.

3.2 | Volumetric wetness probability distributions (objective I)

Tables 3 and 4 highlight that no PP or SNG probability distribution satisfied normality (KS or AD tests), justifying the use of non-parametric statistical tests. May and August distributions had predominantly weak positive skews, whilst October and November had more extreme negative skews (Figure 8). Distributions were principally leptokurtic (displaying excess kurtosis), especially November (Tables 3 & 4). Box-Cox transformations could only normalise (AD tests only) May and August PP distributions, further justifying the non-parametric approach.

3.2.1 | May dataset

During the May sampling date (Figure 9), PP was significantly drier than SNG ($p \leq .001$), with a median θ_v of 27.6% as opposed

TABLE 3 The Kolmogrov-Smirnov (KS) and Anderson-Darling (AD) statistical distribution tests applied to the Permanent Pasture (PP) and Semi-Natural Grassland (SNG) volumetric-wetness probability distributions

| Sampling date | Land-use | Raw data | | | | Box-cox transformed | | | |
|--------------------|----------|-----------|-----------|-----------------|----------|---------------------|-----------|-----------------|----------|
| | | KS | AD | Excess kurtosis | Skewness | KS | AD | Excess kurtosis | Skewness |
| 29th May 2018 | SNG | <0.001*** | <0.001*** | -1.00 | -0.14 | <0.001*** | <0.001*** | -1.02 | -0.11 |
| | PP | <0.001*** | <0.001*** | +0.86 | +0.75 | <0.001*** | 0.839 | +0.02 | -0.00 |
| 2nd August 2018 | SNG | <0.001*** | <0.001*** | +3.20 | +1.39 | <0.001*** | 0.007** | +0.47 | -0.01 |
| | PP | <0.001*** | <0.001*** | -0.04 | +0.25 | <0.001*** | 0.887 | -0.08 | -0.00 |
| 23rd October 2018 | SNG | <0.001*** | <0.001*** | -0.53 | -0.44 | <0.001*** | <0.001*** | -0.86 | -0.13 |
| | PP | <0.001*** | <0.001*** | +4.37 | -1.68 | <0.001*** | 0.013* | -0.49 | -0.14 |
| 29th November 2018 | SNG | <0.001*** | <0.001*** | +7.26 | -2.42 | <0.001*** | <0.001*** | -0.70 | -0.49 |
| | PP | <0.001*** | <0.001*** | +22.58 | -3.72 | <0.001*** | 0.002** | +0.64 | +0.00 |

Note: Note that most tests are extremely significant, indicating that they significantly differ from the Gaussian distribution. The statistical tests are paired with excess kurtosis and skewness values to infer why distributions may violate normality. Box-Cox transformed distributions using the maximum log-likelihood function are shown adjacent to the raw data to highlight the extent of non-normality, with further supporting kurtosis and skewness values. *Significant at the 0.05 probability level. **Significant at the 0.01 probability level. ***Significant at the 0.001 probability level.

TABLE 4 The summary statistics, including arithmetic mean (\bar{x}), median (\tilde{x}), and coefficient of variation (CV), for the volumetric wetness measurements taken at each sampling date within the Permanent Pasture (PP) and Semi-Natural Grassland (SNG)

| Sampling date | Land-use | \bar{x} (θ_v %) | Geometric | Lower | \tilde{x} (θ_v %) | Upper | Max | CV (%) | MWW | BF | |
|--------------------|----------|---------------------------|----------------------|--------------------------|-----------------------------|--------------------------|-----------------|--------|------|-----------|-----------|
| | | | mean (θ_v %) | quartile (θ_v %) | | quartile (θ_v %) | (θ_v %) | | | | |
| 29th May 2018 | SNG | 42.2 | 40.7 | 17.4 | 33.6 | 42.7 | 51.0 | 63.1 | 25.9 | <0.001*** | <0.001*** |
| | PP | 28.2 | 27.8 | 15.9 | 24.6 | 27.6 | 31.2 | 50.2 | 18.5 | | |
| 2nd August 2018 | SNG | 24.7 | 23.6 | 9.3 | 19.6 | 23.4 | 28.3 | 62.4 | 32.1 | <0.001*** | <0.001*** |
| | PP | 30.7 | 30.1 | 12.9 | 26.6 | 30.4 | 34.5 | 51.5 | 18.9 | | |
| 23rd October 2018 | SNG | 45.9 | 44.5 | 14.8 | 38.8 | 46.6 | 54.4 | 65.6 | 23.2 | <0.001*** | <0.001*** |
| | PP | 53.7 | 53.4 | 20.4 | 51.4 | 53.6 | 57.6 | 61.9 | 10.4 | | |
| 29th November 2018 | SNG | 59.2 | 58.9 | 27.3 | 58.3 | 61.0 | 62.5 | 64.7 | 9.2 | 0.757 | <0.001*** |
| | PP | 60.9 | 60.9 | 47.7 | 60.5 | 61.1 | 61.7 | 63.6 | 2.5 | | |

Note: The statistical tests for central tendency (Mann-Whitney Wilcoxon, MWW) and variation (Brown-Forsythe, BF) are also given. Note that all statistical tests are extremely significant, excluding the November MWW test. *Significant at the 0.05 probability level. **Significant at the 0.01 probability level. ***Significant at the 0.001 probability level.

to 42.7% (Table 4: Figure 8). Volumetric wetness differences could be because of higher evapotranspiration within PP, due to the rapidly growing, dense ryegrass sward (Cox, Parr, & Plant, 1988; Hall, 1987). Evapotranspiration is generally assumed to be greater from semi-natural grassland compared to pasture; although this relationship is dependent on vegetation growth and is primarily based off studies involving heather as opposed to 'rush pasture' (Gilman, 2002; Hall & Harding, 1993; Miranda, Jarvis, & Grace, 1984; Orr & Carling, 2006). During May, the SNG plot had several unvegetated soil patches, the moorland grass was heavily grazed and the common rush was withered with minimal foliage, all implying low transpiration rates. Furthermore, the PP plot could additionally contain fewer pockets of impermeable soil as local agricultural practices encourage drainage, reducing θ_V (Wallace & Chappell, 2019).

Removing θ_V variability within a pasture is a central objective of ploughing prior to re-seeding, in order to generate an even grass sward (Schulte et al., 2012). This pioneering study has shown that the PP plot did indeed contain significantly less variation in θ_V ($p \leq .001$) than observed in the SNG plot (Table 4: Figure 8). If the ecological status and functioning of permanent pastures were to be restored to behave more like semi-natural grassland, then the diversity in moisture patterns would need to be re-introduced. As this first sampling date (spring 2018) shows the pasture to be drier than the semi-natural grassland, if representative, this may suggest that permanent pastures dry faster and thus are more

sensitive to water stress with the onset of droughts, a potential concern for livestock production.

3.2.2 | August dataset

Between May and August 2018, the semi-natural grassland saw median θ_V fall from 42.7 to 23.4% (Table 4, Figures 8 & 10). At the 2nd August 2018 sampling date, the API was close to the lowest value for the whole of 2018 (Figure 2), indicating that the sampling programme had observed soil near its driest state in 2018. The high degree of drying was due to relatively high levels of solar radiation over the summer months and moderate rainfall since the previous measurement (only 192 mm in 64 days), with the 40 days prior to sampling recording 56% of the long term average rainfall for this period at this locality (Met Office, 2020). In some contrast, the median θ_V in the PP plot was maintained over the same period, increasing slightly from 27.6 to 30.4% (Table 4, Figure 8). As a result, the SNG plot became significantly drier than the PP plot ($p \leq .001$). As before, the SNG plot contained significantly more variance than the pasture ($p \leq .001$).

The additional drying effects of higher radiation and lower rainfall were more than offset by artificial moisture additions in the form of slurry to the PP field. This indicates that while the PP plot initially

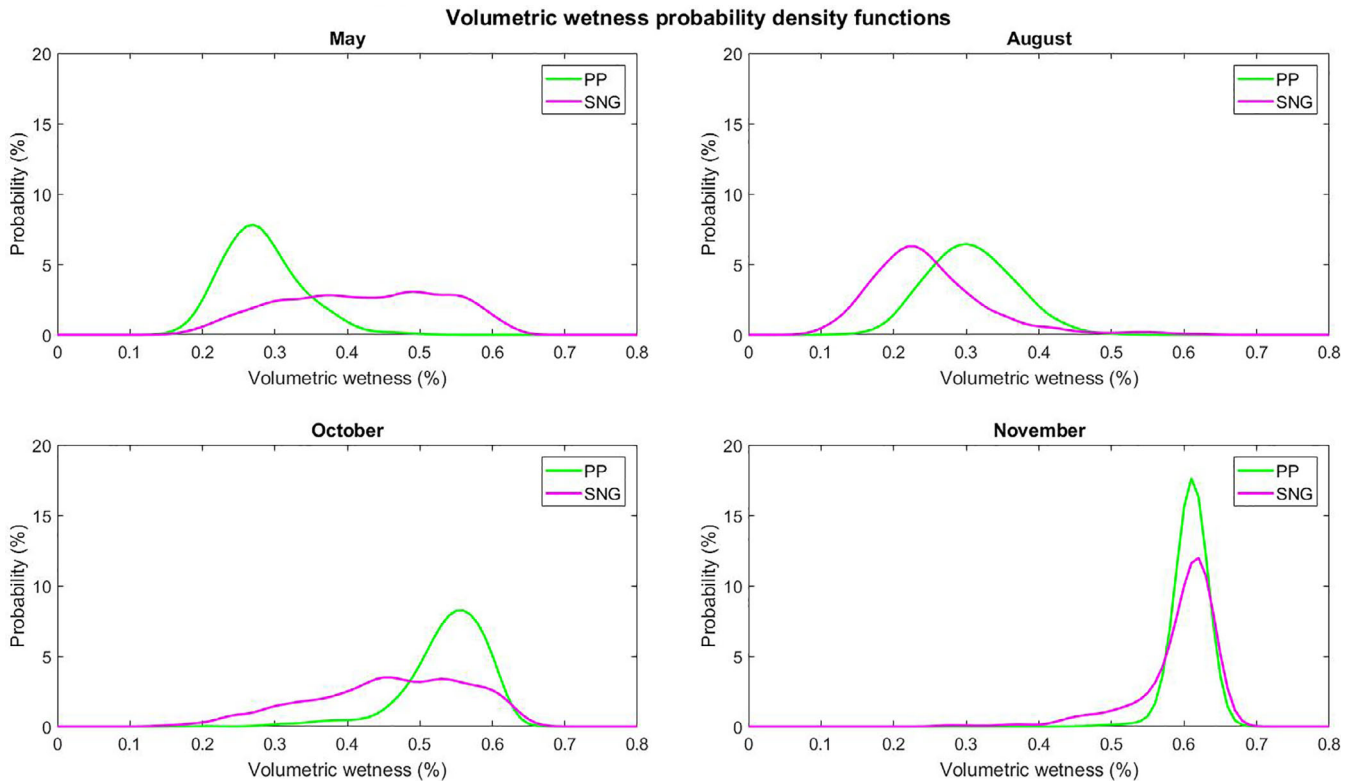


FIGURE 8 The kernel-generated probability density functions for the volumetric wetness during each sampling date. Each distribution was generated according to 768 samples based on the respective land-use. Note that these are statistically tested for normality in Table 3, and the central tendency and variation is statistically compared between land-uses in Table 4

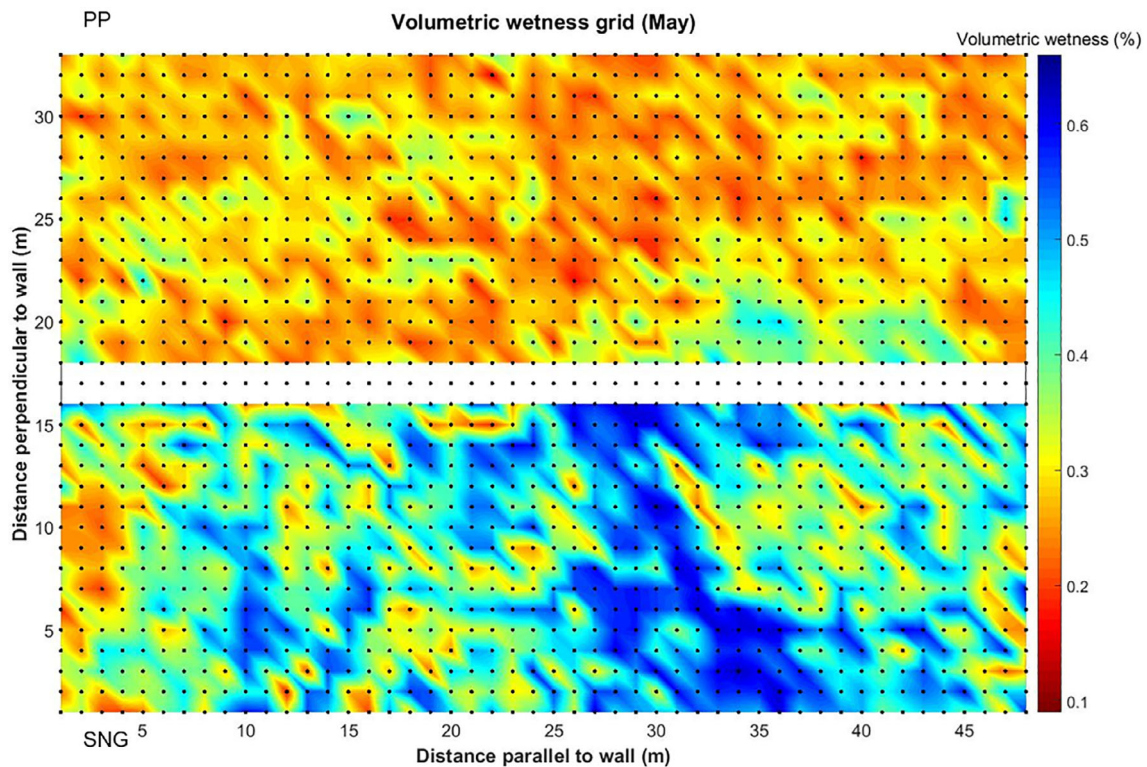


FIGURE 9 The volumetric wetness grid taken on the 29th May 2018. Note that the Permanent Pasture (PP) is at the top of the figure, and the Semi-Natural Grassland (SNG) is at the bottom, with the wall shown to separate the land-uses. The permanent pasture was significantly drier than the semi-natural grassland, and contained significantly less variation. Linear features draining from the south-west to north-east according to the 'regional' topographic highpoint are also evident, primarily within SNG

dried faster than the SNG plot, agricultural interventions could offset these effects. Slurry additions to pastures do have a negative impact on the water quality of adjacent streams however (Hunter, Perkins, Tranter, & Gunn, 1999). Consequently, if such additions were not permitted, then the permanent pasture would lose its artificial moisture input during a drought, and from the May results, could be in a drier state than the semi-natural grassland when the drought is most severe. Withholding slurry during these periods would therefore likely cause substantial sward damage (Schulte et al., 2012).

3.2.3 | October dataset

Over the 81 days between the 2nd August and 23rd October 2018 sampling dates, 504 mm of rain was recorded (Figure 2). As a result, the SNG plot became much wetter, increasing to a median θ_v of 46.6% (Table 4, Figures 8 & 11). The PP plot became wetter still; increasing to 53.6% (Table 4, Figure 8) and remaining statistically wetter than the SNG plot ($p \leq .001$). Interestingly, θ_v within both plots increased by the same amount (+23.2%). Identically to previous sampling dates, the SNG plot contained significantly higher variance ($p \leq .001$).

The October θ_v data show that pastures with summer slurry additions can be wetter than semi-natural grasslands at the onset of autumn rains. Indeed, the median pasture θ_v is only 4.6% below the

median porosity, suggesting that most of the pasture is near saturation and could quickly saturate during storm events. The semi-natural grassland θ_v is 12.9% below median porosity, suggesting some remaining storage capacity before SOF generation. At moisture plots 20 km to the East of those in this study, Ockenden and Chappell (2008) also observed that their single permanent pasture plot was wetter than semi-natural grassland plots during autumnal monitoring.

3.2.4 | November dataset

November sampling (Figure 12) occurred during Storm Diana (28th–29th November 2018) when surface ponding and overland-flow was observed throughout both land-uses. Within the PP plot, overland flow predominantly flowed North by North-East and did not appear to be moving onto SNG (Figure 3). Within the SNG plot, overland flow aligned with the linear drainage patterns and generally headed North-East. Both land-uses contained almost identical θ_v medians ($p \leq .757$), with 61.1 and 61.0%, respectively (Table 4: Figure 8). Variance remained significantly higher in SNG, however ($p \leq .001$: Table 4). Ockenden and Chappell (2008), working at the sites previously mentioned, similarly observed larger θ_v variation within semi-natural grasslands compared to pastures for monitoring dates including the winter.

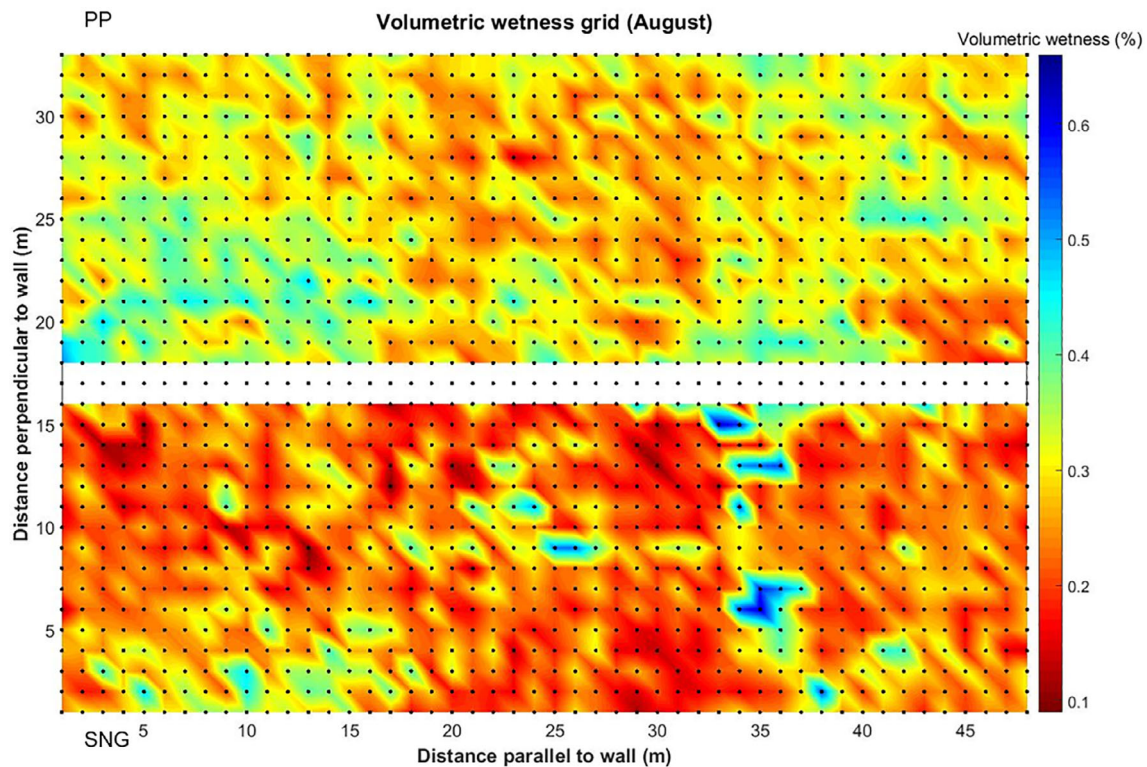


FIGURE 10 The volumetric wetness grid taken on the 2nd August 2018 during the British Isles heatwave. Note that the Permanent Pasture (PP) is at the top of the figure, and the Semi-Natural Grassland (SNG) is at the bottom, with the wall shown to separate the land-uses. The permanent pasture was significantly wetter and significantly less varied than the semi-natural grassland during August sampling. Some linear features are still observable in both land-uses despite the dryness

Between October and November sampling dates, 265 mm of precipitation fell in 36 days, and this was reflected in a very high API on the sampling date (Figure 2). The strong negative skew within both frequency distributions suggests that moisture content at most places in both plots was approaching the upper limit of topsoil wetness, that is, the porosity (Tables 2 & 4; Figure 8; Western et al., 2002). These findings suggest that during large storm events, even semi-natural grasslands may generate SOF and so heighten local flood-risk. Thus attempting to re-establish semi-natural grasslands and associated soils in areas of permanent pasture may not necessarily reduce the incidence of SOF as part of so-called Natural Flood-risk Management.

3.3 | Volumetric wetness spatial structure (objective II)

The geostatistical analysis shows that the spatial structure of θ_v within the SNG plot remained similar (i.e., relatively stationary) from May to November 2018 and is described well by exponential/spherical models (Figure 13; Table 5). Meijles et al. (2003) identically found semi-natural grassland at Dartmoor, UK, to have exponential or spherical semi-variogram models.

The spatial structure of θ_v within PP was similar to that of the SNG plot during the relatively dry conditions of May. Slurry additions and rainfall gradually shifted the spatial structure from exponential to

a Gaussian relationship, whereby the autocorrelation continued beyond the size of the experimental plot (Figure 13). Selected models suitably fit the pasture data, although the October semi-variogram has noticeable residuals at large lags, probably because of the transitioning spatial structure.

The sill is the point at which the semi-variance plateaus within a model (i.e., the semi-variance as lag distance approaches infinity). Most semi-variogram models (Figure 13; Table 5) have a sill marginally above 1, with October PP having a slightly higher sill of 1.31, and November PP (Gaussian model) having a sill at 6.91. The elevated sills outline higher spatial variance of two distantly separated points as the pasture saturated, which was unobserved within SNG (Grayson & Blöschl, 2000).

The effective range is the distance from zero lag to the onset of the sill (95% in exponential models, 100% in spherical and Gaussian models) and can be interpreted as correlation length (i.e., the point beyond which there is no spatial autocorrelation). The effective range within SNG remained essentially stationary throughout the study, suggesting θ_v spatial autocorrelation is independent of the level of saturation. With increased saturation, PP contained considerably larger effective ranges than SNG (Figure 13; Table 5). Agricultural interventions within PP likely homogenised soil variation and facilitated moisture redistribution. As soils saturated, the lack of heterogeneity exerts a greater control on soil moisture redistribution at decimetre scales rather than

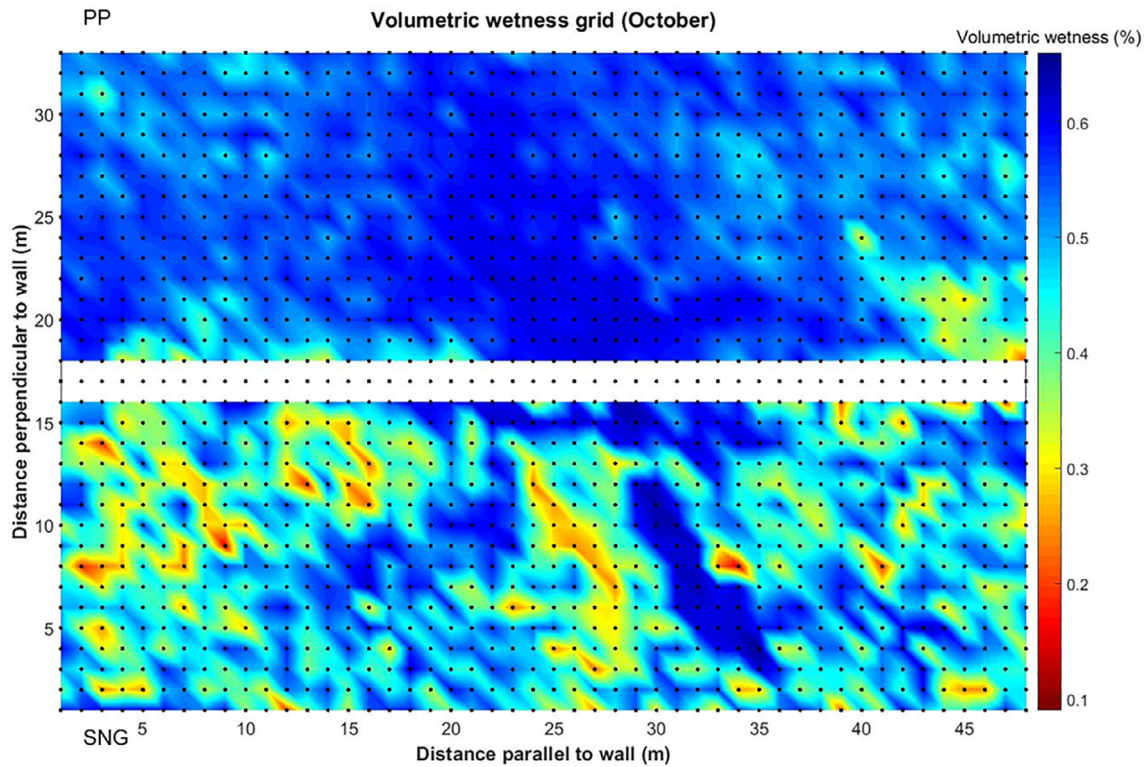


FIGURE 11 The volumetric wetness grid taken during on the 23rd October 2018. Note that the Permanent Pasture (PP) is at the top of the figure, and the Semi-Natural Grassland (SNG) is at the bottom. The wall is shown to separate the land-uses. The pasture was significantly wetter than the semi-natural grassland at the time of sampling, and contained significantly less variation. Linear features are still clearly observable within the semi-natural grassland, although these are slightly masked in the permanent pasture due to the level of saturation

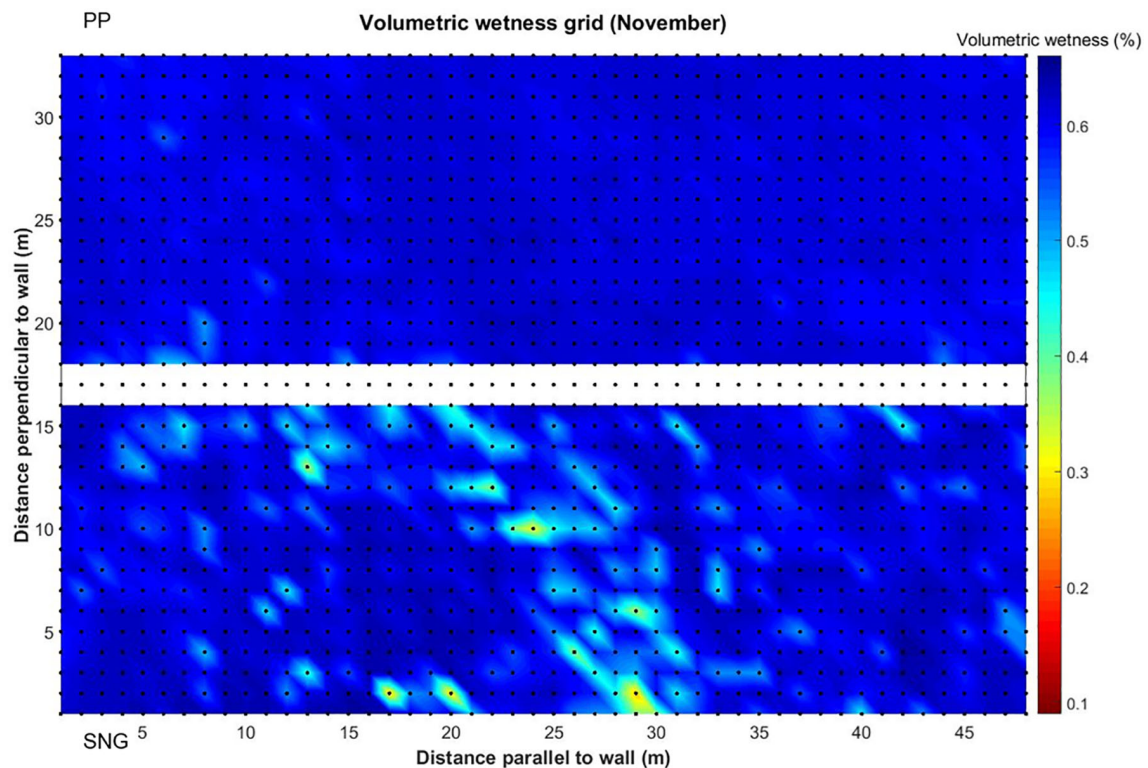


FIGURE 12 The volumetric wetness grid taken on the 29th November 2018 during Storm Diana. Note that the Permanent Pasture (PP) is at the top of the figure, and that the Semi-Natural Grassland (SNG) is at the bottom. The wall is shown to separate the land-uses. Both land-uses have statistically similar medians during these extremely saturated conditions, although SNG remained significantly more varied. Linear features are weakly observable within the semi-natural grassland, even though most of the land-use is at saturation

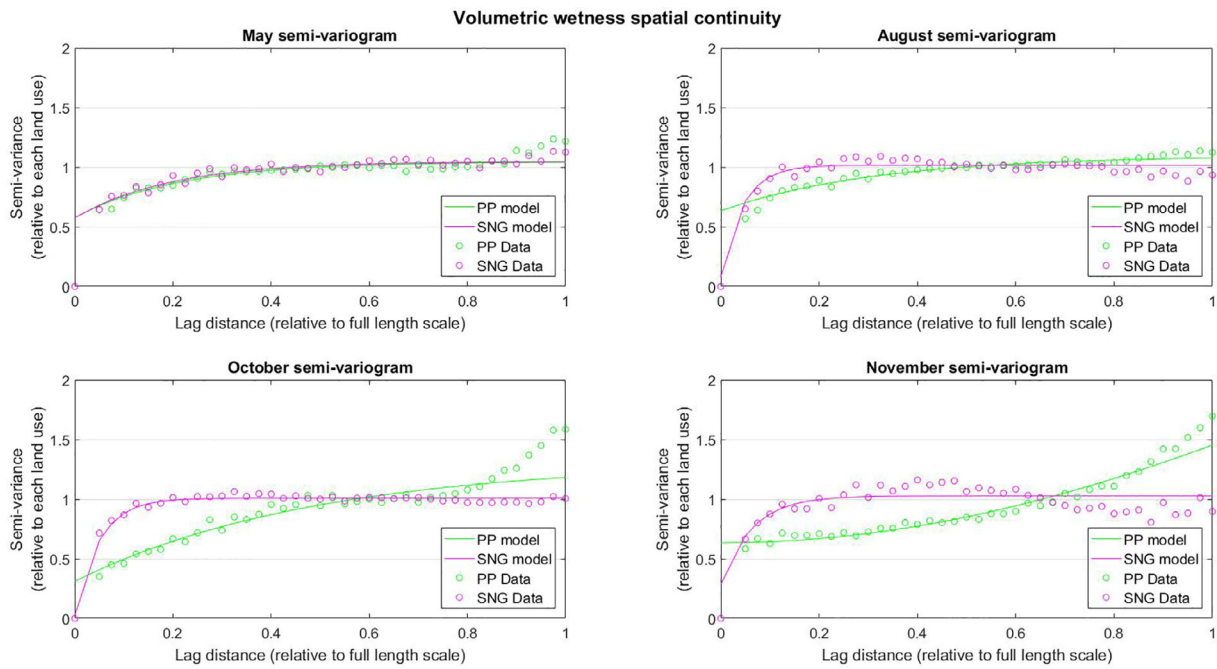


FIGURE 13 The GLOBEC generated empirical semi-variograms for all sampling dates. All models are fitted with the least-squares fit function within GLOBEC, using the 768 samples in each land-use. Note that empirical semi-variograms become progressively dissimilar as the experiment proceeded, and that the full length scale lag distance is 48 m

TABLE 5 The model parameters from GLOBEC generated empirical semi-variogram models for each sampling date, alongside the Antecedent Precipitation Index (API) for each of the respective dates

| Sampling date | API | Land-use | Nugget effect (γ_0) | Sill ($\gamma_0 + P_0$) | Effective range | Model | Residual sum of squares |
|--------------------|-----|----------|------------------------------|---------------------------|-----------------------------|-------|-------------------------|
| 29th May 2018 | 407 | SNG | 0.574 | 1.044 | 0.196 (9.4 m) | Exp | 0.377 |
| | | PP | 0.576 | 1.044 | 0.210 (10.1 m) | Exp | 0.464 |
| 2nd August 2018 | 355 | SNG | 0.045 | 1.017 | 0.141 (6.8 m) | Sph | 0.111 |
| | | PP | 0.635 | 1.097 | 0.317 (15.2 m) | Exp | 0.453 |
| 23rd October 2018 | 524 | SNG | 0.011 | 1.008 | 0.148 (7.1 m) | Sph | 0.085 |
| | | PP | 0.312 | 1.312 | 0.488 (23.4 m) ^a | Exp | 0.643 |
| 29th November 2018 | 611 | SNG | 0.390 | 1.026 | 0.154 (7.4 m) | Sph | 0.370 |
| | | PP | 0.635 | 6.914 | 2.672 (128.3 m) | Gau | 0.575 |

Note: The actual range in metres is given below the effective range. Note that the sill is the nugget plus the partial sill.

^aNote that the model fit is reduced at larger lag distances and, therefore, that the true model effective range is, therefore, highly uncertain.

the metre scales seen with the natural soils under the semi-natural grassland, and thus, amplifies spatial autocorrelation. This was also seen within the decreasing coefficient of variation as PP saturated (Table 4). Ockenden and Chappell (2008) similarly found shorter correlation lengths for semi-natural grassland when compared with those of a single pasture plot. Meijles et al. (2003) found correlation length in semi-natural grassland to vary with saturation, an unobserved process in this study.

The nugget variance is the model semi-variance at zero lag and is generally interpreted as a combination of sampling/instrument error and spatial variation below the minimum sample spacing (i.e., <1 m

variation). Within both PP and SNG plots, the nugget variance reached approximately half that of the sill variance (Figure 13). This would indicate that there is significant variation in θ_V at distances shorter than the 1 m sampling grid. This suggests that future studies that are able to collect more than the 1,536 (i.e., 768×2) values of θ_V across a paired-plot on a sampling day should do so over an even finer sampling resolution (e.g., 10 cm grid). This would confirm whether deterministic spatial structure is present at sub-metre scales or whether other factors such as instrument-related uncertainty in θ_V measurements are responsible. A simulated semi-variogram with 2% θ_V error (uniformly distributed) for a plot-scale grid gave a nugget

variance of approximately 0.05, suggesting instrument-related error is minimal (see Figure S1 and Appendix A). The slightly higher nugget variance in PP compared to SNG suggests increased fine-scale θ_V variation within the pasture, further implying decimetre-scale moisture redistribution.

TABLE 6 The correlations of volumetric wetness with elevation for both the Permanent Pasture (PP) and Semi-Natural Grassland (SNG), as well as when combined, expressed in terms of the correlation coefficient (r)

| Elevation and soil volumetric wetness correlation coefficient (r) | | | |
|---|----------|----------------------|----------------------|
| Month | Land-use | Elevation (land-use) | Elevation (combined) |
| May | PP | -0.107 | -0.453 |
| | SNG | -0.248 | |
| August | PP | 0.124 | 0.223 |
| | SNG | -0.048 | |
| October | PP | 0.140 | 0.194 |
| | SNG | -0.120 | |
| November | PP | -0.099 | 0.000 |
| | SNG | 0.000 | |

Note: Note that inverse correlations imply that higher elevations tend to be drier.

3.4 | Predictor variables of volumetric wetness (objective III)

The final objective of this study is to determine for this particular plot pair, the relative strength of the relationships between soil moisture content and the potential predictors of land-use, elevation, vegetation and season. This was assessed via correlation coefficients and mixed-effects regression modelling.

Table 6 shows the correlation coefficients (r) of θ_V and elevation for both individual and combined PP and SNG plots (Figure 6). Weak correlations between topsoil moisture and elevation for the two plots suggest that elevation is not acting as a dominant control on θ_V (see Figure 3). Combining the weak relationships with the limited topographic range justifies the use of elevation as a random effect in the linear mixed-effects regression model.

Beneath the complex vegetation communities of the semi-natural grassland, differences in θ_V between common rush and grass species were not apparent (Table 7). This may be because of weak vegetation differentiation within the SNG plot, with many sampling grids containing both rush and grass species. Other studies have more successfully differentiated semi-natural grassland vegetation species, with Meijles et al. (2015) outlining that moorland grasses saturate faster than heather or bracken (*Pteridium aquilinum*). Conversely to the SNG plot, soil beneath common rushes in PP was wetter than ryegrass during August and October sampling dates, although similar in May and

TABLE 7 The arithmetic mean (\bar{x}) and median (\tilde{x}) volumetric wetness for ryegrass and common rush within the Permanent Pasture (PP) and Semi-Natural Grassland (SNG) for each sampling date

| Land-use | PP (θ_V %) | | | | | | SNG (θ_V %) | | | | | |
|----------|--------------------|-------------|-----------|-------------|-------------|-------------|---------------------|-------------|----------------|-------------|-------------|-------------|
| | Average | | Ryegrass | | Common rush | | Average | | Moorland grass | | Common rush | |
| Month | \bar{x} | \tilde{x} | \bar{x} | \tilde{x} | \bar{x} | \tilde{x} | \bar{x} | \tilde{x} | \bar{x} | \tilde{x} | \bar{x} | \tilde{x} |
| May | 28.2 | 27.6 | 28.3 | 27.6 | 27.9 | 27.4 | 42.2 | 42.7 | 41.7 | 42.6 | 43.0 | 43.2 |
| August | 30.7 | 30.4 | 30.5 | 30.2 | 35.0 | 34.2 | 24.7 | 23.4 | 24.3 | 23.0 | 25.6 | 24.1 |
| October | 53.7 | 53.6 | 53.5 | 54.5 | 57.2 | 58.8 | 45.9 | 46.6 | 45.8 | 46.4 | 45.9 | 47.0 |
| November | 60.9 | 61.1 | 60.9 | 61.1 | 61.5 | 61.7 | 59.2 | 61.0 | 59.2 | 61.0 | 59.3 | 61.3 |

Note: Both averages are presented due to non-normality in the θ_V distributions.

TABLE 8 The analysis of variance output tables given the most parsimonious linear mixed-effects regression model according to a combination of Akaike and Bayesian Information Criteria using bidirectional elimination

| ANOVA | Df | Sum Sq | Mean Sq | F-value | p-value |
|-----------------|-------|---------|---------|---------|----------|
| Month | 3 | 399,661 | 133,220 | 2,758.4 | <.001*** |
| Land-use | 1 | 28 | 28 | 0.585 | .444 |
| Veg | 4 | 841 | 210 | 4.35 | .002** |
| Month: Land-use | 3 | 78,782 | 26,261 | 543.7 | <.001*** |
| Month:Veg | 12 | 1,257 | 105 | 2.1687 | .011* |
| Residual | 6,094 | | | | |

Note: Note that this includes all fixed effects of the model, where Month: Land-use and Month:Veg indicate interaction terms. *Significant at the 0.05 probability level. **Significant at the 0.01 probability level. ***Significant at the 0.001 probability level.

TABLE 9 The regression model output giving variance (σ^2), slope effects of elevation: month ($\tau_{00 \text{ Elev:Month}}$) and elevation: vegetation ($\tau_{00 \text{ Elev:Vegetation}}$), the intra-class correlation (ICC), the number of elevation values (N_{Elev}), the total number of observations (N_{Obs}), marginal and condition R^2 values, the Akaike Information Criteria (AIC), and the Bayesian Information Criteria (BIC)

| θ_V linear mixed-effects regression model | |
|--|-----------|
| Predictors | Estimates |
| Intercept | 25.93 |
| σ^2 | 48.30 |
| $\tau_{00 \text{ Elev:Month}}$ | 2.55 |
| $\tau_{00 \text{ Elev:Vegetation}}$ | 1.65 |
| ICC | 0.03 |
| N_{Elev} | 38 |
| N_{Obs} | 6,144 |
| Marginal R^2 | 0.777 |
| Conditional R^2 | 0.783 |
| AIC | 41,538 |
| BIC | 41,874 |

Note: The marginal R-squared shows the model fit purely using the fixed-effects, and the conditional R-squared shows the model fit using mixed-effects.

November (Table 7). While the mechanism is unclear, the dense root network beneath common rush apparently retains more moisture (from drainage or transpiration) following slurry or rainfall compared to soil beneath ryegrass.

As a measure of the relative importance of temporal changes (i.e., across the four sampling dates), spatial differences due to land-use (i.e., semi-natural grassland versus agriculturally improved permanent pasture) and vegetation (i.e., common rush versus grass species); linear mixed-effects regression modelling was undertaken and the results presented in Table 8. Both the sampling month ($p \leq .001$) and the vegetation classification ($p \leq .002$) significantly benefit θ_V prediction. The interactions of month-land-use ($p \leq .001$) and month-vegetation ($p \leq .011$) also significantly improve θ_V prediction. The interaction terms in the linear mixed-effects regression model demonstrate that sampling date (i.e., month), significantly affects how land-use and vegetation influence θ_V . Land-use alone does not significantly improve prediction because its importance is already captured within the interaction terms. Modelling results compare well with Meijles et al. (2006) and Meijles et al. (2015), who concluded that vegetation was the dominant control on soil wetness during “dry” conditions at Dartmoor (semi-natural grassland).

The regression model output (Table 9) demonstrates a conditional R^2 of 78.3%, meaning that the predictor variables can explain more than three quarters of θ_V variance at a 1 m resolution. Including elevation only adds a very small additional amount of explained variance (0.6%: the difference between R^2 values), therefore explaining the low intra-class correlation. The degree of interaction between predictor variables seen (i.e., multicollinearity) justifies the use of the mixed-

effects regression model. In particular, the findings highlight the very strong temporal dependency in the predictor variables and the θ_V patterns. The model accuracy is relatable to Meijles et al. (2003) who used slope, topographic index and vegetation as predictor variables in their Dartmoor soil moisture model, explaining 84 and 82% of soil moisture variance for ‘dry’ and ‘wet’ states, respectively.

4 | IMPLICATIONS AND CONCLUSIONS

Grasslands cover 60% of the agricultural area of the United Kingdom. Some 55% of this area is covered by permanent pasture that has a history of ploughing, re-seeding and artificial inputs (e.g., slurry, fertiliser and/or lime). The other grasslands are semi-natural grasslands (in the UK uplands described as ‘moorland’) grazed with sheep and cattle but with near-natural soils largely unaffected by ploughing, re-seeding or artificial inputs.

Despite the areal extent of grasslands in the UK, there is virtually no research contrasting the soil moisture differences between permanent pastures and the less intensively managed semi-natural grasslands. This study, while focused on one experimental plot-pair in Cumbria (upland UK), has demonstrated the intensity of moisture measurements required to highlight the new research needed to explain the contrasting behaviour between pasture and semi-natural grassland if the whole landscape is considered.

The key findings were:

- The contrast in soil moisture patterns between the paired plots changed markedly throughout the monitoring period, as did the interactions between the potential controlling variables. During spring sampling (29th May 2018), the pasture was significantly drier than the semi-natural grassland, making the vegetation more sensitive to water stress. With the reduced rainfall and higher transpiration of summer, the moisture content of the semi-natural grassland plot reduced to only 23%. In some contrast, moisture added in the form of cattle slurry maintained topsoil moisture at ~30% in the pasture, underlining an overlooked agronomic benefit of slurry. As these slurry additions have consequences for water quality, a desire to restore wildlife habitats could see this practice barred. As the pasture was significantly drier than the semi-natural grassland prior to slurry additions, such a change could amplify the drying of pasture soils during drought conditions. Research is needed to demonstrate how dry pastures could become without slurry additions, and whether soil restoration techniques could successfully moderate such conditions. The smaller dataset of dry bulk density and porosity did indicate that the pasture may have been compacted by agricultural practices. Such new research might therefore include intensive sampling of soil properties and subsequent modelling of the combined factors to show their role in the moisture status of pastures during droughts (and indeed during floods). Additional hydrological variables, such as infiltration capacity, evapotranspiration, and hydraulic roughness, would further improve system interpretation.

- With the onset of autumn storms, the slurry-wetted pasture continued to be wetter than the semi-natural grassland, being much closer to saturation (i.e., 4.6% vs. 12.9% below saturation, respectively). These wetter antecedent conditions could mean that such pastures saturate quicker and consequentially produce more of the rapidly moving Saturation-excess Overland Flow, and so heighten downstream flood risk. Experimental research is needed to quantify if a greater mean wetness of slurry-managed pasture soils in the autumn does translate into a greater incidence, magnitude and speed of SOF. Given the extensive nature of permanent pastures in the high rainfall areas of upland UK, experimental research into measures that would reduce the incidence, magnitude and speed of SOF (arising from saturated topsoil conditions) on or immediately downslope of pastures is also needed. Such work would need to combine paired moisture plots and volumetric overland-flow measurements. Visual observations during a storm event during high antecedent moisture conditions (29th Nov 2018) did show that the largely saturated semi-natural grassland did generate overland flow. This underlines the importance of new detailed measurements of soil moisture and overland flow in both pasture and adjacent moorland conditions, so as not to assume that moorland restoration will completely remove overland flow incidence as part of 'Natural Flood-risk Management' interventions (see Kirkby & Morgan, 1980 for overland flow quantification).
- The high intensity of soil moisture sampling in the paired plots highlighted the linear connectivity of zones of wetter soils in the semi-natural grassland (in a SSW–NNE direction) that was 'smeared out' within the pasture as a result of the history of ploughing, re-seeding, land drainage, etc. This may explain the much longer correlation lengths and stronger spatial-structure observed for the pasture, especially at increased moisture contents. This highlights how farming and changes in floristic/faunal composition have altered the hydrological diversity of an area. The high proportion of semi-variance at the smallest measurement separation (i.e., 1 m) demands further research conducted at even smaller separation distances (e.g., 0.1 m). This would determine if the cause is the presence of deterministic spatial structure at sub-1 m distances or intrinsic errors in the moisture measurement technique. Significantly increasing the sampling intensity above that used in this study (i.e., 1,536 moisture measurement per plot pair) would make it difficult to sample the whole area without the average moisture content having changed over the duration of the sampling period. Potentially, multiple moisture probes would need to be used synchronously for each plot pair, and each probe used cross-calibrated.

The paired-plot experimental design with a dense grid of soil moisture measurements has provided clear evidence for a contrasting soil moisture regime between intensively managed pasture versus the semi-natural soil vegetation conditions prevailing at the studied upland locality in Cumbria (UK); and that the relationship changes markedly through the year. The detailed story of within-plot behaviour acts as a basis for detailed replication to understand plot-scale

variability across the landscape. The challenge is to replicate this work at numerous locations in this mountainous region to understand which of the contrasts observed in one plot-pair dominates in this landscape. Of equal importance is the extensive replication of the work in other very different locations of permanent pasture in the UK and overseas. Given the limited viability of plot scale representativeness at the landscape scale, a body of further research is required before results and conclusions can be applied to regional-scale models.

ACKNOWLEDGEMENTS

The authors appreciate land access from the Lonsdale Estate Trust and the tenant farmer. We acknowledge the contribution of field assistants, and gratitude is due to Vassil Karloukovski, Ann Kretzschmar, John Quinton, Annette Ryan and Ben Surridge for equipment and laboratory access. The project was funded by the European Regional Development Trust Fund and the Eden Rivers Trust as part of CGE Project 50, with NERC grant NE/R004722/1 providing some analytical support, including use of Environmental Agency data.

CONFLICT OF INTEREST

The authors declare no conflicts of interest.

DATA AVAILABILITY STATEMENT

The data that support the findings of this study have been made available at: <https://dx.doi.org/10.17635/lancaster/researchdata/331>.

ORCID

Ethan E. Wallace  <https://orcid.org/0000-0003-2314-4667>

REFERENCES

- Agriculture and Horticulture Development Board (AHDB). (2013). *Management and control of common (soft) rush* (pp. 1–6). Kenilworth, UK: Agriculture and Horticulture Development Board.
- Albertson, K., Aylen, J., Cavan, G., & McMorrow, J. (2009). Forecasting the outbreak of moorland wildfires in the English Peak District. *Journal of Environmental Management*, 90, 2642–2651.
- Bates, D. M., Maechler, M., & Bolker, B. (2012). lme4: Linear mixed-effects models using Eigen and R. (version 0.999999-0) [R]. R.
- Beven, K.J., & Germann, P. (1982). Macropores and water flow in soils. *Water Resources Research*, 18, 1311–1325. <https://doi.org/10.1029/wr018i005p01311>.
- Brown, M. B., & Forsythe, A. B. (1974). Robust tests for the equality of variances. *Journal of the American Statistical Association*, 69, 364–367.
- Bengtsson, J., Bullock, J. M., Egoh, B., Everson, C., O'Connor, T., O'Farrell, P. J., ... Lindborg, R. (2019). Grasslands—More important for ecosystem services than you might think. *Ecosphere*, 10, 1–20.
- Bonell, M., & Williams, J. (1986). The generation and redistribution of overland flow on a massive oxic soil in a eucalypt woodland within the semi-arid tropics of North Australia. *Hydrological Processes*, 1, 31–46.
- Chappell, N. A., & Ternan, L. (1992). Flow path dimensionality and hydrological modelling. *Hydrological Processes*, 6, 327–345.
- Cooper, A. H., Rushton, A. W. A., Molyneux, S. G., Hughes, R. A., Moore, R. M., & Webb, B. C. (1995). The stratigraphy, correlation, provenance and palaeogeography of the Skiddaw group (Ordovician) in the English Lake District. *Geological Magazine*, 132, 185–211.

- Chu, D. (2017). *The GLOBEC Kriging Software Package: EasyKrig3.0. (Version 1)*. Falmouth, MA: Woods Hole Oceanographic Institution Mathworks.
- Cox, R., Parr, T. W., & Plant, R. A. (1988). Water use and water-use efficiency of perennial ryegrass swards as affected by the height and frequency of cutting rate. *Grass and Forage Science*, 43, 97–103.
- Department for Environment, Food and Rural Affairs (DEFRA). (2019). *Agriculture in the United Kingdom 2018* (p. 5). London: Department for Environment, Food and Rural Affairs (DEFRA)
- Drewry, J. J., Littlejohn, R. P., & Paton, R. J. (2000). A survey of soil physical properties on sheep and dairy farms in New Zealand. *New Zealand Journal of Agricultural Research*, 43, 251–258.
- Dunne, T., & Black, R. D. (1970). An experimental investigation of runoff production in permeable soils. *Water Resources Research*, 6, 478–490.
- Environment Agency (EA). (2019). *Hydrometric data*. Retrieved from www.environment.data.gov.uk/hydrology/
- Entekhabi, D., Rodriguez-Iturbe, I., & Castelli, F. (1996). Mutual interaction of soil moisture state and atmospheric processes. *Journal of Hydrology*, 184, 3–17.
- Gaskin, G. J., & Miller, J. D. (1996). Measurement of soil water content using a simplified impedance measuring technique. *Journal of Agricultural Engineering Research*, 63, 153–160.
- Gaugemap. (2019). *Wet Sleddale*. Retrieved from www.gaugemap.co.uk/#/Map/Summary/7716/3029
- Gilman, K. (2002). *Modelling the effect of land use change in the upper severn catchment on flood levels downstream*. Peterborough, UK: English nature.
- Grayson, R., & Blöschl, G. (2000). *Spatial patterns in catchment hydrology*. Monash University, Victoria: Cooperative Research Centre for Catchment Hydrology.
- Hall, R. L. (1987). Processes of evaporation from vegetation of the uplands of Scotland. *Transactions of the Royal Society of Edinburgh: Earth Science*, 78, 327–334.
- Hall, R. L., & Harding, R. J. (1993). The water use of the Balquhider catchments: A processes approach. *Journal of Hydrology*, 145, 285–314.
- Hayhow, D. B., Eaton, M. A., Stanbury, A. J., Burns, F., Kirkby, W. B., Bailey, N., ... & Symes, N. (2019). *The state of nature*. The state of Nature partnership, London: State of Nature Partnership.
- Holden, J., Shotbolt, L., Bonn, A., Burt, T. P., Chapman, P. J., Dougill, A. J., ... Worrall, F. (2007). Environmental change in moorland landscapes. *Earth Science Reviews*, 82, 75–100.
- Holland, J. E., Bennett, A. E., Newton, A. C., White, P. J., McKenzie, B. M., George, T. S., ... Hayes, R. C. (2018). Liming impacts on soils, crops and biodiversity in the UK: A review. *Science of the Total Environment*, 610–611, 316–322.
- Hunter, C., Perkins, J., Tranter, J., & Gunn, J. (1999). Agricultural land-use effects on the indicator bacterial quality of an upland stream in the Derbyshire Peak District in the UK. *Hydrological Research*, 33, 3577–3586.
- Jarvis, R. A., Bendelow, V. C., Bradley, R. I., Carroll, D. M., Furness, R. R., Kilgour, I. N. L., & King, S. J. (1984). *Soils and their use in northern England*. Harpenden, UK: Soil survey of England and Wales.
- Kain, R. J. P., Chapman, J., & Oliver, R. R. (2004). *The enclosure maps of England and Wales, 1595–1918*. Cambridge: Cambridge University Press.
- Kirkby, M. J., & Morgan, R. P. C. (1980). *Soil erosion*. Chichester: Wiley.
- Lamarque, P., Tappeiner, U., Turner, C., Steinbacher, M., Bardgett, R. D., Szukics, U., ... Lavorel, S. (2011). Stakeholder perceptions of grassland ecosystem services in relation to knowledge on soil fertility and biodiversity. *Regional Environmental Change*, 11, 791–804.
- Macleod, C. J. A., Humphreys, M. W., Whalley, W. R., Turner, L., Binley, A., Watts, C. W., ... Haygarth, P. M. (2013). A novel grass hybrid to reduce flood generation in temperate regions. *Scientific Reports*, 3, 1683.
- Magliano, P. N., Mindham, D., Tych, W., Murray, F., Nosetto, M. D., Jobbágy, E. G., ... Chappell, N. A. (2019). Hydrological functioning of cattle ranching impoundments in the dry Chaco rangelands of Argentina. *Hydrological Research*, 50, 1596–1608.
- Marshall, M. R., Francis, O. J., Frogbrook, Z. L., Jackson, B. M., McIntyre, N. R., Reynolds, B., ... Wheater, W. S. (2006). The Pontbren catchment study: A multi-scale experimental programme investigating the impact of UK upland land use on flood risk. In *9th BHS national hydrology symposium* (pp. 85–90). Durham: BHS.
- Marshall, M. R., Francis, O. J., Frogbrook, Z. L., Jackson, B. M., McIntyre, N., Reynolds, B., ... Chell, J. (2009). The impact of upland management on flooding: Results from an improved pasture hillslope. *Hydrological Processes*, 23, 464–475.
- McCorry, M. J., & Renou, F. (2003). *Ecology and management of Juncus effusus (soft rush) on cutaway peat*. Dublin: Forest Ecology Research Group.
- McIntyre, N., & Marshall, M. R. (2010). Identification of rural land management signals in runoff response. *Hydrological Processes*, 24, 3521–3534.
- Meijles, E. W., Williams, A. G., Ternan, J. L., & Dowd, J. F. (2003). Runoff generation in relation to soil moisture patterns in a small Dartmoor catchment, Southwest England. *Hydrological Processes*, 17, 251–264.
- Meijles, E. W., Williams, A. G., Ternan, J. L., Anderson, J. M., & Dowd, J. F. (2006). The influence of grazing on vegetation, soil properties and stream discharge in a small Dartmoor catchment, Southwest England, UK. *Earth Surface Processes and Landforms*, 31, 622–631.
- Meijles, E. W., Dowd, J. F., Williams, A. G., & Heppell, C. M. (2015). Generation of storm runoff and the role of animals in a small upland headwater stream. *Ecology*, 8, 1312–1325.
- Met Office. (2020). *UK climate averages*. Retrieved from www.metoffice.gov.uk/public/weather/climate/gcwn4cte6
- Miller, J. D., Gaskin, G. J., & Anderson, H. A. (1997). From drought to flood: Catchment responses revealed using novel soil water probes. *Hydrological Processes*, 11, 533–541.
- Minet, J., Laloy, E., Lambot, S., & Vanclooster, M. (2011). Effect of high-resolution spatial soil moisture variability on simulated runoff response using a distributed hydrological model. *Hydrology and Earth System Science*, 15, 1323–1338.
- Miranda, A. C., Jarvis, P. G., & Grace, J. (1984). Transpiration and evaporation from heather moorland. *Boundary Layer Meteorology*, 28, 227–243.
- Morse, A. (2019). *Early review of the new farming programme*. London: National Audit Office.
- Ockenden, M. C., & Chappell, N. A. (2008). The effect of topography, sub-surface strata and land-use on observed distributions of soil moisture within a sub-catchment of the river Eden, Cumbria. In *10th BHS national hydrology symposium* (pp. 202–207). BHS: Exeter.
- O'Connell, P. E. O., Beven, K. J., Carney, J. N., Clements, R. O., Ewen, J., Fowler, H., ... Tellier, S. (2004). *Review of impacts of rural land use and management on flood generation*. London: DEFRA.
- Orr, H. G., & Carling, P. A. (2006). Hydro-climatic and land-use changes in the river lune catchment, north West England, implications for catchment management. *River Research and Applications*, 22, 239–255.
- Pan, W., Boyles, R. P., White, J. G., & Heitman, J. L. (2012). Characterizing soil physical properties for soil moisture monitoring with the North Carolina environment and climate observation network. *American Meteorological Society*, 29, 933–943.
- R Core Team. (2018). *R: A language and environment for statistical computing*. Vienna, Austria: R Foundation for statistical computing.
- Sansom, A. L. (1999). Upland vegetation management: The impact of overstocking. *Water Science and Technology*, 39, 85–92.
- Schulte, R. P. O., Fealy, R., Creamer, R. E., Towers, W., Harty, T., & Jones, R. J. A. (2012). A review of the role of excess soil moisture conditions in constraining farm practices under Atlantic conditions. *Soil Use and Management*, 28, 580–589.
- Stone, P. (2007). *Bedrock geology UK north: An explanation of the bedrock geology map of Scotland, northern England, Isle of Man and*

- Northern Ireland—1:625,000 (5th ed.). Keyworth: British Geological Society.
- United States Department of Agriculture (USDA). (1999). *Soil taxonomy: A basic system of soil classification for making and interpreting soil surveys*. Washington DC: USDA.
- Wallace, E. E., & Chappell, N. A. (2019). Blade aeration effects on near-surface permeability and overland-flow likelihood on two stagnosol pastures in Cumbria, UK. *Journal of Environmental Quality*, 48, 1766–1744.
- Western, A. W., Grayson, R. B., & Blöschl, G. (2002). Scaling of soil moisture: A hydrologic perspective. *Annual Review of Earth and Planetary Sciences*, 30, 149–180.
- Whalley, W. R. (1993). Considerations on the use of time-domain reflectometry (TDR) for measuring soil moisture content. *Journal of Soil Science*, 44, 1–9.
- Wheater, H., Reynolds, B., McIntyre, N., Marshall, M. R., Jackson, B. M., Frogbrook, Z. L., ... Chell, J. (2008). *Impacts of upland land management on flood risk: Multi-scale modelling methodology and results from the Pontbren experiment*. Manchester: DEFRA.
- Whyte, I. (2006). Parliamentary enclosure and changes in landownership in an upland environment: Westmorland, c1770-1860. *Agricultural History Reviews*, 34, 240–256.
- World Reference Base (WRB). (2015). *World reference base for soil resources 2014*. Rome: FAO.
- Zehe, E. R., & Blöschl, G. (2004). Predictability of hydrologic response at the plot and catchment scales: Role of initial conditions. *Water Resources Research*, 40, W10202.

SUPPORTING INFORMATION

Additional supporting information may be found online in the Supporting Information section at the end of this article.

How to cite this article: Wallace EE, Chappell NA. A statistical comparison of spatio-temporal surface moisture patterns beneath a semi-natural grassland and permanent pasture: From drought to saturation. *Hydrological Processes*. 2020; 1–21. <https://doi.org/10.1002/hyp.13774>

APPENDIX A: NUGGET VARIANCE ASSOCIATED WITH MOISTURE-PROBE

A simulated semi-variogram with 2% θ_v error (identical to the soil moisture-probe) was generated over a grid of equal-scale to the plots used in this study, with the error uniformly distributed. This simulated semi-variogram was used to assess the impact of the moisture-probe uncertainty on semi-variogram model parameters. The actual range in metres is given below the effective range. Note that the sill is the nugget plus the partial sill. This table should be used alongside Figure S1, and compared with Table 5 and Figure 13.

| Semi-variogram | Nugget effect (γ_0) | Sill ($\gamma_0 + P_0$) | Effective range | Model | Residual sum of squares |
|----------------|------------------------------|---------------------------|-----------------|-------|-------------------------|
| Simulated | 0.045 | 1.002 | 0.072 (3.5m) | Sph | 0.028 |